2013

Non-local interactions in spatial evolutionary games

Ozgur Hakan Aydogmus
Iowa State University

Non-local interactions in spatial evolutionary games

by

Ozgur Hakan Aydogmus

A dissertation submitted to the graduate faculty
in partial fulfillment of the requirements for the degree of
DOCTOR OF PHILOSOPHY

Major: Applied Mathematics

Program of Study Committee:
Zhijun Wu, Major Professor
Karin Dorman
Anastasios Matzavinos
Alexander Roitershtein
Paul Sacks

Iowa State University
Ames, Iowa
2013

DEDICATION

To my parents Mustafa and Nuran, and my wife Melike.

TABLE OF CONTENTS

LIST OF TABLES

LIST OF FIGURES

ACKNOWLEDGEMENTS

I would like to express my thanks to those who helped me with various aspects of conducting research and the writing of this disertation.

First, I would like to thank my advisor, Dr. Zhijun Wu for his guidance and support throughout this work. I also want to thank Dr. Wen Zhou for his support and patience and being around at every step of this study.

I would also like to express my deep gratitude to my committee member: Dr. Alexander Roitershtein for his continuous support in probability theory.

I also want to thank my committee members for their efforts and contributions to this work: Dr. Paul Sacks, Dr. Anastasios Matzavinos, Dr. Karin Dorman.

Finally, I would like to thank all of my friends here in Ames for their support, especially to Aysel Saricaoglu for her suggestions and comments.

ABSTRACT

As a special case of symmetric game in which the players share a common payoff matrix, evolutionary game provides a suitable approach to model and explore the emergence of cooperative behavior in natural and social systems. The evolutionary spatial game (ESG) further specifies the payoff for each individual by both the payoff matrix M and the spatial dependence structure of the population on a geophysical domain. Two players game serves as a foundation of modeling various biological/social interactive systems and provides a great amount of interesting game theoretical models such as prisoner's dilemma game, snow drift game etc.

We formulate a two players evolutionary spatial game under the framework of initialization, effective local payoff, and the Markov chain for strategy update. The spatial dependence structure is modeled by a probability distribution parameterized by the dependence geometry and strength in the neighborhood of each location. Particularly, we study the structure based on Gaussian process. Computational methods are proposed and applied to study the convergence of simulations. In addition, limiting non-local differential equation is introduced and analysed in terms of spreading speeds and traveling waves.

CHAPTER 1. OVERVIEW

Evolutionary game theory is a model used to understand the dynamics of a population in a strategic setting. This modeling approach requires a population of individuals, rules of the game and an interaction structure. Here, rules of the game is given by a fitness/payoff matrix. On the other hand, interaction rules may vary. It is possible to consider a population of individuals, for example, with kin selection [43], age structure [8], spatial interaction [33] or time delay [26]. Dynamical behavior of each structure may be different from each other.

In this study, we mainly focus on the game Prisoner's Dilemma and the evolution of cooperation played among a population of spatially interacting individuals. Here, we aim to show that spatial structure gives rise to evolution of cooperation in finite and infinite populations with long range interactions. Both, simulations of finite population games and their deterministic limit favors cooperation in some parameter region.

1.1 Game theory

Prisoner's Dilemma game is one of the best known games in social and life sciences. The game helps us model cooperative and defective individuals and it has been a rich source of research since 1950s. The backstory of the game is as follows:

Two people have committed a crime together and have been caught. Criminals I and II are being held in separate cells and both are offered a deal by the police. They have to decide what to do independently. Essentially, the deal is this:

- If I confesses and II denies taking part in the crime, I goes free and II goes to prison for ten years.
- If II confesses and I denies participating in the crime, I goes to prison for ten years and II goes free.
- If both I and II confess, each will serve six years in prison.

- If both I and II deny taking part in the crime, each goes to prison for 1 year.

The payoff matrix of this game with column and row players being I and II, respectively, is given by

	Confess	Deny
Confess	(6,6)	(10,0)
Deny	(0,10)	(1,1)

A rational or selfish player should confess regardless of opponent's strategy. Thus, confess is the Nash equilibrium (discussed in section 1.1.1) of this game. However, it is clear that if both chose to deny, both serve short prison sentences.

Here the strategy "deny" represents cooperation (C) with the partner and "confess" represents defection (D). The modeling approach is realistic and it is not surprising that defection would be the first choice of rational individuals. Despite this fact, how can we explain that cooperation arises among individuals, organisms, animals or societies? We seek an answer to this question in the context of evolutionary game theory. Thus, we consider a population of individuals playing a two-strategy game on a spatial domain. In the following two sections, a brief introduction to simultaneous and evolutionary game theories will be provided.

1.1.1 Simultaneous games

Game theory is concerned with situations in which players interact with one another, and the payoff of each individual depends on both his/her and the opponents' choice of strategy. In this section, we consider only the games played by two individuals simultaneously. Thus, payoffs are given by a payoff matrix M. Suppose both players have the same set of strategies denoted by $S = \{s_i | i = 1, ...n\}$. Then, the interpretation of m_{ij} is the payoff of a player playing strategy s_i against the other player with strategy s_j. This is the game with pure strategy players. It is also possible to consider players with mixed strategies. For example a player can choose to play a certain strategy s_i with a probability p_i. In population games, mixed strategies naturally arise since a proportion of the population plays a certain strategy.

Mixed strategies are used to define mixed Nash equilibriums. The concept of Nash equilibrium is useful to analyze simultaneous games. It is also connected to rest points of the corresponding dynamical system which will be introduced in the next section.

We define the idea of best response as the best (pure or mixed) strategy of one player, given information about the strategy choice of the other player. The type of the information depends on the game played. For example, in the Prisoner's Dilemma game, strategy choices of players depend on their past. If one trusts his/her opponent, s/he is very likely to cooperate with him/her. Here we consider the payoff matrix as the only information known by the players. Therefore, a player searches for the best response to his opponent's strategy according to the given information.

To make this precise, introduce the notation. Say s and t are two strategies chosen by player I and II, respectively. We write $M_i(s,t)$, $i = I, II$ for the payoff of corresponding player. We say strategy s is a best response to strategy t if s produces as good payoff as any other strategy paired with t. i.e.

$$M_I(s,t) \geq M_I(s_{-1},t)$$

for all other strategies s_{-1} of player I. Now we can define Nash equilibrium.

Definition 1.1.1. We say that the pair of strategies (s,t) is a Nash equilibrium if s is best response to t and t is best response to s.

This definition is natural for rational players since they respond each strategy to maximize their benefits. The equilibrium concept is also natural. If the players choose best responses to each other's strategy then no one will change his/her strategy.

1.1.2 Evolutionary games

The assumption of rational players in game theory is not needed in population games. Evolutionary game theory shows that the basic ideas of game theory can be applied to settings in which individuals can exhibit different forms of behavior such as unconscious choice of strategy. The theory is mostly applied to evolutionary biology. The idea of Maynard Smith and Price [49] is that the genes mostly determine the observable characteristic of an organism. Thus the fitness of an individual depends largely on genes. More fit organisms produce more offsprings and, hence, these genes dominate the population.

The fitness of an organism is not independent of its environment. Therefore, its interactions with other organisms have to be considered, which is the reason why we use a game theoretic framework. Here, an organism's characteristic and behaviors can be considered as its strategy.

In addition, its fitness which depends heavily on the strategies of other players can be considered as the payoff.

Evolutionary stable strategy (ESS) for a population game is another important concept. Given the game, some Nash equilibriums are evolutionary stable strategies if the population playing ESS cannot be invaded by small population of mutants. In the next subsection, we will explain these concept in the language of dynamical systems.

1.1.2.1 Stochastic evolution and its deterministic limit

Consider a population of N individuals playing a game with payoff matrix M and strategy set S. Here we define the population dynamics as a Markov birth-death chain $X_n = (X_n^i)_{i\in S}$ where X_n^i denotes the frequency of individuals playing the strategy i in the population. Suppose at each time step, an individual is randomly chosen to change his/her strategy. Then, the payoff of this player is given by $p_i = (MX_n)_i$. The transition probabilities depend on the payoff matrix and the state of the population at the current time step. For example, the probability that an individual with strategy j changes his strategy to i can be given by

$$P\big[X_{n+1}^i = x^i + \frac{1}{N} | X_n^i = x^i\big] = \frac{1}{2} + \frac{p_i - p_j}{2\Delta p}$$

where Δp denotes the maximum payoff difference. This rule is defined in [53] and is called as replicator rule, since its mean field equations are the famous replicator equations [20] given by

$$\dot{\rho}_i = \rho_i \sum_{k=1}^{n} m_{il}\rho_l - \sum_{k,l=1}^{n} m_{kl}\rho_i\rho_k\rho_l$$

where ρ_i denotes the frequency of individuals playing strategy i. Different probabilities give rise to different ODE systems. The convergence of trajectories of the Markov chains and ODEs is justified in [5]. The same result is also valid for continuous time birth-death chains.

Replicator equations constitute the most favorable model in evolutionary game theory, since its asymptotical behavior characterizes the game itself. In particular, the stable rest point of the dynamical system corresponds to the Nash equilibriums. The following theorem explains the relationship between game theory and the above defined ODE.

Theorem 1.1.2. *[20] Consider the game with the payoff matrix M and corresponding replicator equation. Then following are true.*

- *If x_0 is a Nash equilibrium of the game then x_0 is a rest point of replicator equation.*

- *If x_0 is Lyapunov stable then it is a Nash equilibrium of the game.*
- *If x_0 is asymptotically stable rest point of replicator equation then it is an ESS of the game.*

1.2 Overview of this thesis

In the second chapter, we generalize the above defined Markov chain to a lattice population. Interactions between individuals are modeled by discrete Interaction kernels. Four different microscopic update rules (transition probabilities) are generalized using non-local interaction kernels and simulated. Frequency of cooperators are presented as a function of game parameter and the variance of the kernel. These simulation results suggest that the small variance of the kernel favors cooperation. In addition these four rules are compared statistically. For a parameter region including all four biologically important 2×2 games, simulations are repeated for one microscopic rule. It is conjectured that as the variance gets larger, frequencies obtained from the simulations converges to mean field equations.

In the third chapter, we introduce the mesoscopic limiting integro-differential equation of replicator rule using the theory developed in [23]. The basic properties of the equation such as quasi-monotonicty and linear determinacy are given. Parameter region is identified for Prisoner's Dilemma game. Using these properties, existence of traveling wave solutions has been shown combining the theories developed in [46, 6]. Moreover, the existence uniqueness and comparison principle is proved in whole parameter space for Prisoner's Dilemma game. Using the squeezing technique [2] along with the comparison principle, asymptotic speed of spread of the non-local equation is studied in the same parameter region. The relationship between asymptotic speed and traveling wave speed is given. As a result, it is shown that cooperation is an ESS if the speed of the moving frame is large or small enough.

CHAPTER 2. SPATIAL GAMES WITH GAUSSIAN STRUCTURES

2.1 Introduction

Emergence of cooperative behavior in natural and social systems is a major challenge in a variety of scientific disciplines such as biology, sociology or economics [15, 12, 32]. Game theoretical approaches have been proposed and proven to be suitable and efficient to study this issue. An evolutionary game model approaches the interactions of individuals in a population by a fitness/payoff matrix. In general, the payoff of an individual depends on entries of the fitness/payoff matrix and the spatial structure of the underline population. This spatial dependence structure can be modeled by a conditional probability distribution by which an individual collect information from its neighborhood. Naturally, this structure also influence the microscopic update rule of strategies, which defines a transition probability of a birth death process. At each generation, some or all agents may alter their strategies depending on payoff of each individual in the neighborhood and synchronism or asynchronism of the microscopic update rules adapted. Transition probabilities are based on the known rules and also depend on the local payoff in the neighborhood of the individuals under discussion. In this study we focus on the effects of the spatial structure under different asynchronous update rules.

In many biological systems such as mycobacterium, fungi, plant, and animals, it is natural to have individual behavior distance dependent. It is, therefore, natural to model the evolutionary games by considering non-uniform interactions among individuals, i.e. interactions among individuals are functions of displacement or distance between them. Distance dependent weights in modeling network have been studied widely such as in the application of neural networks. In the context of lattice domain, distance dependent interactions via dispersal or competition kernels have been studied in seed dispersal [10, 51, 13], and in spread of diseases [1]. Nonlocal interactions can also be modeled by a variety of kernels with certain biological applications [9].

Here we propose a model via spatially weighted payoff calculation and interactions on a

lattice with periodic boundary conditions in the context of evolutionary games. Spatial weights has been modeled by discrete Gaussian weights and size of the neighborhood depends closely on the standard deviation of the kernel, which is also the diffusion coefficient in heat kernel. Individuals collects payoffs from their neighbors according to the weights and the payoff matrix. We focus on the prisoner's dilemma game and four widely used microscopic update rules: best take over (BTO), Moran (M), replicator (R), and Fermi-Dirac (F) update rules. The effect of the deviation of the kernel on the evolution of cooperation under these rules will be considered via simulations. These four update rules are compared by using the Latin square design, which is a classical statistical experimental design to account variations. Moreover, convergence to the mean-field equation for larger values of the standard deviation will be concluded from the simulations for general, 2×2 symmetric games.

The Chapter is organized as the following. In section 2.2, we give some preliminaries to describe a given kernel and usage of these weights for calculation of payoff values. We also introduce generalizations of four update rules and connections of these rules with the previous work. In section 2.3, we consider Prisoner's Dilemma game and provide comparisons between simulations of different update rules and uniform and Gaussian kernels. In addition Latin square method is used to show differences between these rules. In section 2.4, S-T plane simulations are performed considering different standard deviations of the kernel using one of the update rules given in section 2.2. Section 2.5 concludes the study and gives future research directions.

2.2 Previous study

Symmetric two players games are the most studied games in evolutionary game theory. They can be described by the payoff matrix

$$M = \begin{pmatrix} R & S \\ T & P \end{pmatrix},$$

where each component of the M represents the payoff received by the row player against the column player. Conventionally, the first row player is referred to as the cooperator and the second one is referred to as the defector.

Simulations of the games can be performed in $S - T$ plane by restricting the parameters S and T to the intervals $-1 < S < 1$, $0 < T < 2$ and taking $R = 1$ and $P = 0$ [45]. The plane regions $\{(S,T)|S > 0, T < 1\}$, $\{(S,T)|S < 0, T > 1\}$, $\{(S,T)|S > 0, T > 1\}$,

and $\{(S,T)|S < 0, T < 1\}$ corresponds to the Harmony, the Prisoner's dilemma (PD), the Snowdrift and the Stag-Hunt games, respectively. In addition, each of the above games can be represented with one parameter. For the Prisoners Dilemma game, we adopt the one parameter family given by $R = 1$, $T = b$, $S = P = 0$ due to [35] in section 3.

The classical approach of evolutionary game theory assumes uniform distribution over the population under consideration. Thus, population is well mixed and dynamic can be modeled by an ordinary differential equation under large population limits. The most favorable model is the replicator equation [20] which is the mean field equation of what we call replicator rule. In addition, the other two probabilistic rules considered in this chapter are Moran and Fermi rules having different mean field equations, with similar dynamical behavior [53]. In well-mixed populations, asymptotic density of cooperators are zero for Prisoner's Dilemma game and 1 for the harmony game. Snow-Drift game and the Stag-Hunt game accept a third equilibrium point which is stable in the case of the former one and unstable in the case of the later.

More realistic spatial dynamics of evolutionary game theory was first studied by Nowak and May [36]. They considered the Prisoners Dilemma game using the one parameter family given above. They showed that cooperation can be maintained in this game on a two dimensional grid with the nearest neighbor uniform interactions using deterministic update rule called best take over. The following work of Nowak and May [35] considered synchronous and asynchronous probabilistic update rules again assuming each player interacts with their immediate neighbors. Regular grid models are more realistic than the mean field model since the assumption made for spatial games considers spatial distance dependent interactions. However, regular grid with immediate neighbor interactions does not reflect the effect of long range interactions. Small-world networks models this property. Evolutionary games on these networks were studied by Shang et al. [47]. They considered weights as a probability distribution depending on distance between individuals with the assumption that each individual interacts with a constant number of player. It is also possible to generalize population structure using graph theoretical arguments. In general, evolutionary game dynamics on weighted graphs has been studied by Lieberman et al. [28]. They extended the structure of population considering a non-homogeneous population on a graph by using Birth-Death and Death -Birth processes described in Outsuki et al. [39]. This structure models different aspects of evolutionary games such as time dependent weights [7], and updating neighborhoods [27]. Lastly, distance based weights for evolutionary games via long tailed discrete dispersal kernels have been considered by Muneeperakul et al. [34] on

river networks.

Above mentioned generalized proportional update rules and pairwise comparison rules will be adapted to our model in section 2.3. The most commonly used examples of the former rules are Moran and best takes over rules. The later group includes Fermi rule and replicator rule. Using these rules, many studies explored the effects of the spatial structure on emergence and maintenance of cooperation. They concluded that population structure often promotes cooperative behavior [37] (for exception in the Snow Drift game see [17] on above defined graph structures.) Effect of neighborhood shape has been studied extensively by Hauert [16]. In addition, a recent study by Szamado et al. [52] explores the effect of dispersal and neighborhood size in evolutionary games and concludes that spatially explicit version of evolutionary games can overcome the exception in the Snow-Drift game. Roca et al. [45] studied influence of above mentioned probabilistic update rules in $S-T$ plane both on graphs and 2-D lattice.

Thus, it can be seen that there is no rigorous study and comparison of lattice dynamics for these four rules considering long range interactions. We model long range interactions using discrete dispersal kernels. Contrary to existing studies, we consider interaction range and weights as a factor affecting the lattice dynamics in addition to payoff values. This factor has been measured by the variance of the kernel in consideration. The model set up and modification of the transition probabilities for these four rules are given in the next section.

2.3 Model development for evolutionary spatial games (ESG)

The ESG is a temporal-spatial process that defines a spatial distribution of population or strategies on geophysical domain Ω at each time point t. The collection of all individuals at each location defines a random matrix $\mathbf{Z}_t$. This matrix evolves along time with some jumping distribution $P(\mathbf{Z}_t|\mathbf{Z}_{t-1}, \mathbf{Z}_{t-2}, \cdots, \mathbf{Z}_0)$ which can be either a regular probability distribution or a degenerate measure. We consider the pure strategy game that each geophysical location is occupied or adapts only one species or one strategy, i.e $\mathbf{Z}$ is a collection of binary random variables such that $\mathbf{Z} \in \{0,1\}^{|\Omega|}$.

ESG specifies that the jumping distribution is a function of payoff of populations at the current stage and history. For each location, given the temporal information and spatial neighborhoods, we can compute the payoff of the individual at the location and update its status accordingly. In this study, we focus on asynchrony rules that one location is updated at each

time point. We, therefore, refer the jumping distribution as microscopic update rule.

To have a well-defined model of ESG, we need to specify the update rules, the individual payoff at each location, and $\mathbf{Z}_0$. Hence, the modeling of ESG is decomposed into three parts: initialization, local payoff computation, and microscopic update. Initialization is the step to specify the initial configuration of the populations geophysically; local interaction is the step of computing the local effective payoff of the focal location and its relevant neighbors, by which we apply the microscopic update rule to proceed the game dynamics along time. Step 1 and 2 specify the spatial structure while step 3 defines temporal dynamics relying on some probability structures (regular or degenerate ones).

2.3.1 Initialization

Initialization specifies the initial configuration (distribution) of the interacting population spatially at the initial time. In practice, the initial configuration of interacting species for observational study is always missing variable.However, for the purpose of *in silico* experiment the starting time point can always be pre-specified, at which the state of system is reasonable to be considered as the initial configuration.

On a geophysical domain Ω, the initial configuration is one of the $2^{|\Omega|}$ combinations $\{0,1\}^{|\Omega|}$ where 0 and 1 denote defector and cooperator respectively. We denote the initial configuration by

$$D_0(\{0,1\}^{|\Omega|}) = \{Z(s,0) \in \{0,1\} \mid \text{for all } s \in \Omega\} \tag{2.3.1}$$

where location $s = (k,l)$ with $k,l \in \mathbb{Z}^+$ for lattice model under consideration. It is pointed out that the equilibrium distribution of the populations may depend on the initial configuration for certain types of update rules in [36, 35]. This demonstrates that the initial distribution might have some effects on the equilibrium distributions. To be more specified, we focus on three interesting initial configurations, where each has some biological implications:

1. well-mixed model: $Z(s,0) \sim \ i.i.d.$ Binary(1/2) which may correspond to hypothetical initial configuration for observational study or the experimental study of cooperative organisms like mycobacterium;

2. well separating model: the populations of species (e.g., cooperators and defectors) on Ω are comparable and are separated by regular curves like straight lines or circles spatially,

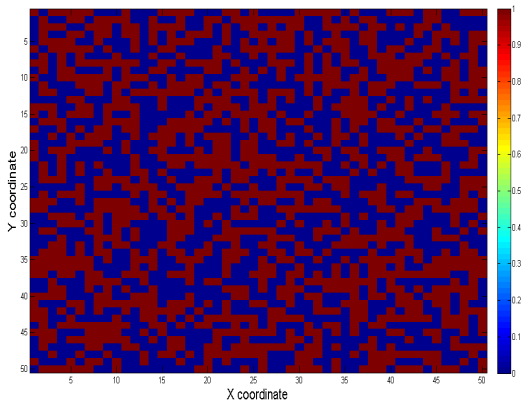

(a) Well mixed model, empirical frequency of defector (red one) is 0.4948.

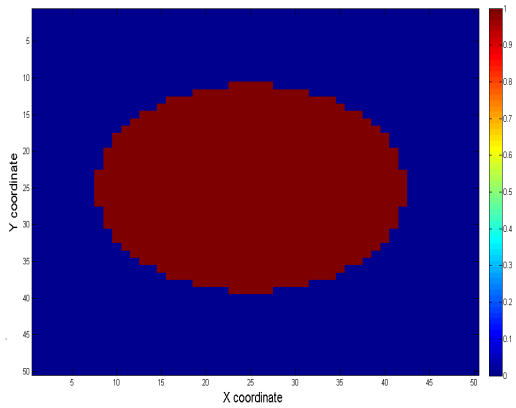

(b) Well separating model, empirical frequency of defector (red one) is 0.31

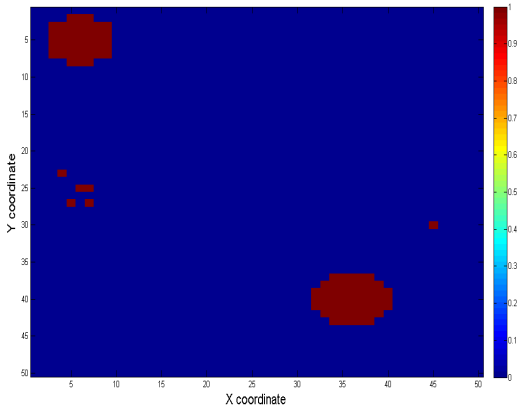

(c) Invasion model configuration, empirical frequency of defector (red one) is 0.0392

Figure 2.1 Interesting initial configurations of ESG.

this may correspond to the behavior of immune system and foreign pathogens in chronic disease such as granuloma in *Tuberculosis*;

3. invasion model: one of the two populations dominates another one, the introduced attempt to invade the "sea" of the dominating one by one or several small groups while the contact boundary might be irregular, this may correspond to many ecological case for newly introduced species (passive or active) such as introducing house finch into North America in 1940s, and introducing wild European rabbit into Australia in 18th century. It also can be used to model immunobiological problem such as invasion of bacteria/protozoa to host or epidemiological problem such as spreading of diseases, etc.

Figure 2.1 demonstrates these three cases with three examples.

2.3.2 Effective local payoff

Given initial configuration, the classical game dynamics direct each individual or species occupying certain location/cell on domain/lattice domain to update its status based on its own fitness and the average fitness related to its payoff. Motivated by [36, 37], the effective payoff for each individual is not simply the matrix component due to the spatial structure, but a collective payoff via interacting with all the locations other than itself or its local neighborhoods. Hence, denote effective payoff of individual at location $(k,l) \in \Omega$ at time t by $\pi(Z(k,l,t))$, where $Z(k,l,t) \in \{0,1\}$ is the type of species or strategy, we have

$$\pi(Z(k,l,t)) = \int_{(k,l)^c} M(Z(k,l,t), Z(x,y,t)) d\mu(x,y) \tag{2.3.2}$$

for some pairwise payoff function $M(\cdot,\cdot)$ and σ-finite measure μ.

For ESG defined on the lattice, (2.3.2) can be further specified as

$$\pi(Z(k,l,t)) = \sum_{(x,y)\in N_{kl}} M(Z(k,l,t), Z(x,y,t)) K_{kl}(k,l,x,y) \tag{2.3.3}$$

where the neighborhood of (k,l) is given by

$$N_{kl} = \{(i,j) \in \Omega \mid ||(k,l) - (i,j)|| \leq r\}. \tag{2.3.4}$$

Here $K_{kl}(k,l,x,y)$ is the Radon-Nikodym derivative of μ with respect to the counting measure restricted on the lattice. $M(Z(k,l,t), Z(x,y,t))$ gives the value of payoff matrix in accordance with the strategies $Z(k,l,t)$ and $Z(x,y,t)$ being realized.

In this work, we assume that the procedure of computing effective payoff using K is weakly stationary. In other words, $K_{kl}(k,l,x,y)$ depends only on the displacement or distance between (k,l) and (x,y) so that $K_{kl}(k,l,x,y) = K(k,l,x,y) = K(k-l, x-y)$ or $K_{kl}(k,l,x,y) = K(k,l,x,y) = K(|k-x|, |l-y|)$ where the later case is much stronger by assuming isotropic.

We define $K(k,l,x,y)$ as the information kernel that captures how each location summarize the information it collects at time step t from its closest neighbor and distant individuals. For example, if $K(k,l,x,y)$ is uniform [36, 37], i.e.

$$K(k,l,x,y) = \frac{1}{N_{kl}}$$

the individual at location (k,l) will consider all neighbors equally important; if $K(k,l,x,y)$ is symmetric like multivariate t-distribution density or multivariate normal density, then, the

individual at (k,l) collect more information from nearest neighborhood than the further ones without bias on the direction of contact. If $K(k,l,x,y)$ is asymmetric like multi-dimensional Gamma distribution density [11], the neighbors may contribute to or influence location (k,l) in a different way according to the displacement. By using asymmetric kernel, one can also model the transport process in ESG.

In this study, we particularly focus on $K(k,l,x,y)$ in the form of a Gaussian process for some spatial dependence structure V , i.e.,

$$K(k,l,x,y) = \frac{1}{\sqrt{2\pi \cdot \det(V)}} \exp\left(-\frac{1}{2}((k-x),(l-y))V^{-1}((k-x),(l-y))'\right). \tag{2.3.5}$$

If V is not diagonal matrix, then kernel (2.3.5) also provides asymmetric shape to collect information.

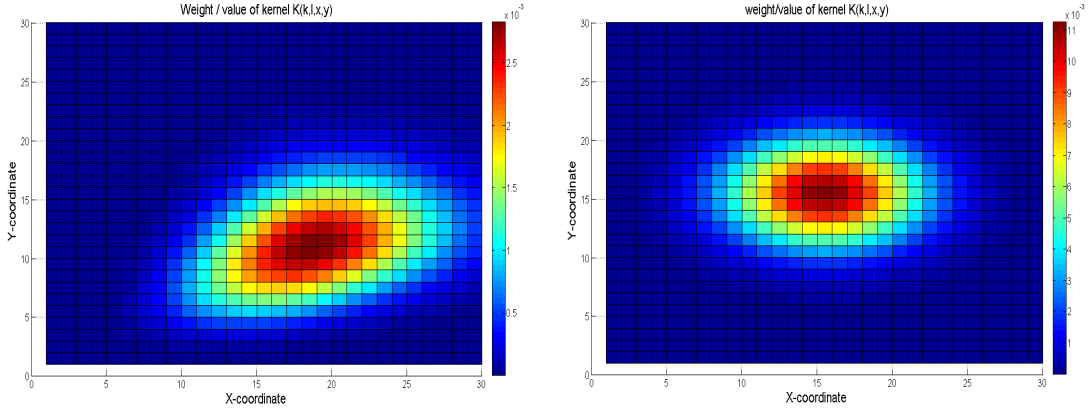

(a) Kernel $K(k,l,x,y)$ defined by bivariate Gamma density centering at the location (k,l).

(b) Kernel $K(k,l,x,y)$ defined by bivariate normal density centering at the location (k,l).

Figure 2.2 Weights assigned to all neighborhoods for the focal (k,l), which are the values of $K(k,l,x,y)$.

Notice (2.3.5) is nothing but the *p.d.f.* of the bivariate normal distribution so that V serves as the covariance matrix where its diagonal components model the variability of the information collection. On the other hand, (2.3.5) is the heat kernel which provides interpretation of information collection procedure as a diffusion process. Hence, V models the diffusion coefficient in heat equation if V is diagonal that one can interpret the information collection as mobility of the individual as well. Particularly, if $V = \sigma^2 I$, we expect that K approaches to uniform kernel as $\sigma \to \infty$ and the system is frozen if $\sigma \to 0$ which results in K approach δ-measure on each location.

2.3.3 Microscopic Update Rules

Equipped with (asynchrony) microscopic update rules, the ESG model is a Markov chain defined on $\{0,1\}^{|\Omega|}$ that can be described as the following:

Step 1. Uniformly sample location (k,l) on Ω

Step 2. Sample opponent location (x,y) in N_{kl} for (k,l) using Gaussian process

Step 3. Compute the effective local payoff for each location

Step 4. Compute jumping probability P using quantities from Step 3

Step 5. Update the strategy for location (k,l)

Step 6. Repeat these steps independently

The most commonly used generalized proportional update rules are Moran rule (M) for $n=1$ and Best take over rule (BTO) for $n=\infty$ where

$$P(Z(k,l,t+1)=z(x,y,t)|Z(x,y,t))=\frac{\left(\sum\limits_{(u,v)\in N_{kl}}\pi(z(u,v,t))K(k,l,u,v)\delta_{\{(x,y),(u,v)\}}\right)^n}{\left(\sum\limits_{(u,v)\in N_{kl}}\pi(z(u,v,t))K(k,l,u,v)\right)^n} \tag{2.3.6}$$

Another commonly used family of update rules is pairwise comparison rules which are completely determined by two locations:

$$P(Z(k,l,t+1)=z(x,y,t)|Z(x,y,t))=\omega F(\pi(z(k,l,t))-\pi(z(x,y,t))) \tag{2.3.7}$$

where ω is a normalizing constant. Here $F(s)=1/2+s/\Delta s$ gives replicator rule (R) and $F(s)=[1+\exp(Ts)]^{-1}$ gives Fermi rule (F) where Δs is the maximum payoff difference.

Markov property of the microscopic update rules:

$$\begin{aligned}
&P(Z(k,l,t+1)=1|C_t,C_{t-1},\cdots,C_1)\\
=&P(Z(k,l,t+1)=1|C_t)\\
=&P(Z(k,l,t+1)=1|Z(x,y,t))P((x,y)\text{ is selected}|(k,l)\text{ is selected})P((k,l)\text{ is selected})\\
=&P(Z(k,l,t+1)=1|Z(x,y,t))\int_{N_{kl}}K(k,l,u,v)\delta_{x,y}d\mu(u)\otimes d\nu(v)\cdot\frac{1}{N^2}\\
=&\frac{1}{N^2}P(Z(k,l,t+1)=1|Z(x,y,t))K(k,l,x,y)
\end{aligned}$$

2.3.4 Summary

In this section, we summarize update rules defined above and connect these rules to previous studies. Consider a population on a 2D grid and a probability distribution $f(||x||)$ on the plane where $||.||$ is the euclidean norm in the plane and σ denotes the deviation of the distribution. Spatial weights are basically determined by discretization of the given probability distribution on the grid Thus weight of the link (i, j) is given by

$$k(i,j) = \int_{i-0.5}^{i+0.5} \int_{j-0.5}^{j+0.5} f(||x-y||)\, dx\, dy.$$

In the case of $f(||x||) = \frac{1}{2\pi\sigma^2} \exp(-\frac{||x||}{2\sigma^2})$ we get discrete version of Gaussian kernel which can be represented as a weight matrix and is isothermal due to symmetry of the metric. This definition of discrete kernel is consistent with the one defined in equation (2.3.5) [48]. In this study, we use a family of truncated Gaussian Kernels. Here σ measures the effect of distance. As σ goes to infinity, this effect vanishes and we get uniform distribution on the lattice. If σ goes to zero, we get Dirac-delta distribution. Thus, the size of the neighborhood closely depends on the value σ which determines the support of the kernel on the lattice.

We consider an analog of payoff calculation for adaptively weighted networks studied in [7]. An individual i interacts with others depending on the value of σ. Denote the neighborhood of the individual as $\Lambda(i, \sigma) = \Lambda(i)$. For a given interaction kernel k, the payoff of an individual can be calculated as

$$\Pi_i = \sum_{j \in \Lambda(i)} k(i,j) s_i^T M s_j$$

where $s_i^T = (1, 0)$ if i uses strategy 1 and $s_i^T = (0, 1)$ if i uses strategy 2.

Next we define four update rules. Moran and Best take over rules are special cases of the proportional update rules. Thus, let's start with defining this rule. Let Π_i be the payoff of individual i in the present time step. For a fixed value of σ, neighborhood is given by $\Lambda(i)$. The probability that an agent i, with strategy s_i, imitates its neighbor j, with strategy s_j, is given by

$$P\{s_i \to s_j\} = \frac{\sum_j (k(i,j)\Pi_j \delta_{s(i),s(j)})^n}{(\sum_{j \in \Lambda(i)} k(i,j)\Pi_j)^n}.$$

In the case of $n = 1$, the transition probability is the same as the transition rule defined by [7]. On the other hand, if we take uniform weights, this rule is exactly the proportional update rule mentioned above and equivalent to the rule defined by Nowak et al. in [35]. In the case

of $n = 1$ we call this rule as generalized Moran rule (M). In addition, generalized best take over rule (BTO) can be described by the limiting case of this probability as n goes to infinity. Thus, i adopts the strategy of j, if $k(i,j)\Pi_j = \max_{l\in\Lambda(i)}\{k(i,l)\Pi_l\}$. Again in the case of uniform interaction in a small neighborhood, we get the best takeover rule studied by Nowak [35].

Other two rules are special cases of what we call pairwise comparison rules. One individual is chosen for reproduction and one of its neighbor is chosen for death. The transition probabilities of these rules explicitly depend on payoff difference of these two individuals and the distance between them. Thus, the probability that an agent i, with strategy s_i, replaces its neighbor j, with strategy s_j, is given by

$$P\{s_i \to s_j\} = w_{ij}F(\Pi_i - \Pi_j).$$

Here F is a function determining the update rule. As in the classical approach, we call this rule as Fermi rule if $F(s) = [1 + \exp(Ts)]^{-1}$ and replicator rule if $F(s) = \frac{1}{2} + \frac{s}{\Delta s}$. Here w_{ij} is a function of distance between these individuals. In our simulations, w_{ij} is taken as total weight of sites with the same weights. Thus, in the case of uniform interaction in a neighborhood, we will get the classical Fermi and replicator rules. For the Fermi rule similar modifications exits. See the review paper [40] for details, and its applications in learning theory in which w_{ij} is described as strength of influence.

2.4 Study of ESG based on simulation of PD games

We use discrete lattices with individuals at each site. They adopt either cooperation or defection as their strategies. In our model, individuals can interact with all players in their neighborhood, the size of which depends on the kernel deviation σ, and collect their payoffs according to the weights. Since we use asynchronous dynamics at each time step a randomly selected individual i and its neighbors play the game and i updates his strategy according to transition rules described above. Here, extended and weighted neighborhood definition helps us to simulate the dynamics with long range interactions. In the case of Von Neumann and Moore neighborhoods of classical cellular automata, the kernel is given by uniform distribution in a small neighborhood. However, it is more realistic to assume interaction or influence between individuals increases when they are close to each other. The study by [45] considers effect of Euclidean distance in a network environment, yet they assumed interactions limited to four or eight neighbors. In this study, we assume interaction range on the lattice determined only by

the deviation of the kernel. In addition, interactions and information collection are weighted according to the discretized kernel. In particular, an individual gets more payoff from a close neighbor than a far away individual and if the distance between two individuals are close they are more likely to imitate each other. From a mathematical perspective, the probability of imitating a close neighbor is greater than the probability of imitating a far away neighbor assuming that both have the same payoff.

In all simulations through the paper, we use 50×50 discrete lattices with periodic boundary conditions. Initial configurations obtained via randomly initialized population of $N = 2500$ sites adopting one of the possible strategies cooperation or defection. Initially, each site adopts one of the two strategies with the same probability unless otherwise stated. The links between individuals are determined by the distance between them via the dispersal kernel. If the distance between two individuals is greater than r, the weight of this link between them is taken as 0 where r is the smallest integer greater than 5σ. This assumption is crucial in terms of computational easiness. In addition, it is also a reasonable assumption since Gaussian kernels are thin tailed. At every time step, each individual plays the game with others, gathers its payoff, and using one of four update rules, a chosen individual updates its strategy according to one or all its neighbors calculated payoffs. We let the system run $2N \times 10^4$ step, enough for convergence of dynamics to stationary mean for $\sigma < 3.5$ as shown in the next subsection. Color maps given in this section describe the population mean in the $\sigma - b$ or $r - b$ planes for Gaussian or uniform distributions, respectively.

2.4.1 Convergence of Simulation of ESG

It was proposed that the number of iterations for convergence might be $10^4 N^2$ in [14]. The microscopic update rules, however, may differ by the number of iterations for convergence. In addition, for the games favoring coexistence, no criteria for convergence have been established.

We use sample frequency to capture the first moment of process. Second moment captures dependence structures of the game, e.g., clustering or random mixed. For each block of 1250 time points, we compute the largest eigenvalue of the sample covariance matrix as an estimator of the second moment. Time series for the two statistical estimates for replicator and Fermi rules are shown below.

In this subsection, we use simulations for some parameter values and different update rules to check the convergence of the Markov processes whose transition probabilities are given by

the three stochastic update rules defined above. We take the parameter values from the sets $\Sigma = \{1, 2, 3\}$ and $B = \{1.25, 1.50, 1.75\}$. For this discrete set of parameters $\Sigma \times B$, using Latin square experimental design each update rule is connected to three pair of parameters in this plane and simulated the games for this parameter values except for the values in reverse diagonal elements in the following table.

σ/b	1.25	1.50	1.75
1	F	R	
2	M		R
3		M	F

History of the processes has been saved to get time series data. To check the stability of mean, mean density of the population of cooperators is calculated and saved at every 1250 time steps. In addition, we use approximation of semi-variogram parameters, sill and range again using 1250 as the windows size.

To construct the covariance matrix, spatial data in each window of size 1250 time steps has been saved as a vector and the covariance matrix of this resulting 2500×1250 matrix is calculated. The largest eigenvalue of the matrix has been considered as the parameter for the spatial dependence of individuals.

To study how spatial dependence changes over time and describe spatial variability, we will consider a_t and s_t, range and sill respectively see [44]. Fix the time t and suppose that we have the configuration L_t at this time. Given two locations s_i and s_j, variogram is defined for random variables $Z(s_i)$ and $Z(s_j)$ as

$$2\gamma(s_i - s_j) = var\{Z(s_i) - Z(s_j); \forall s_i, s_j \in L_t\}$$

and the function γ is called the semi-variogram. We used spherical semi-variogram model to estimate the parameters a_t and s_t. The range a_t is the distance at which semi-variogram reaches a maximum. In other words, it is an estimation of the distance h beyond which $Z(s + h)$ and $Z(s)$ are no longer correlated. The sill s_t is the value of the semi-variogram evaluated at any distance greater than or equal to range. Note also that another parameter for semi-variogram is nugget. However, in our model nugget has to be chosen as zero since at each node of the lattice there is just one strategy and $\gamma(0) = 0$. It is also a possibility to use spatio-temporal variogram model to fit the time series data using both space and time lags.

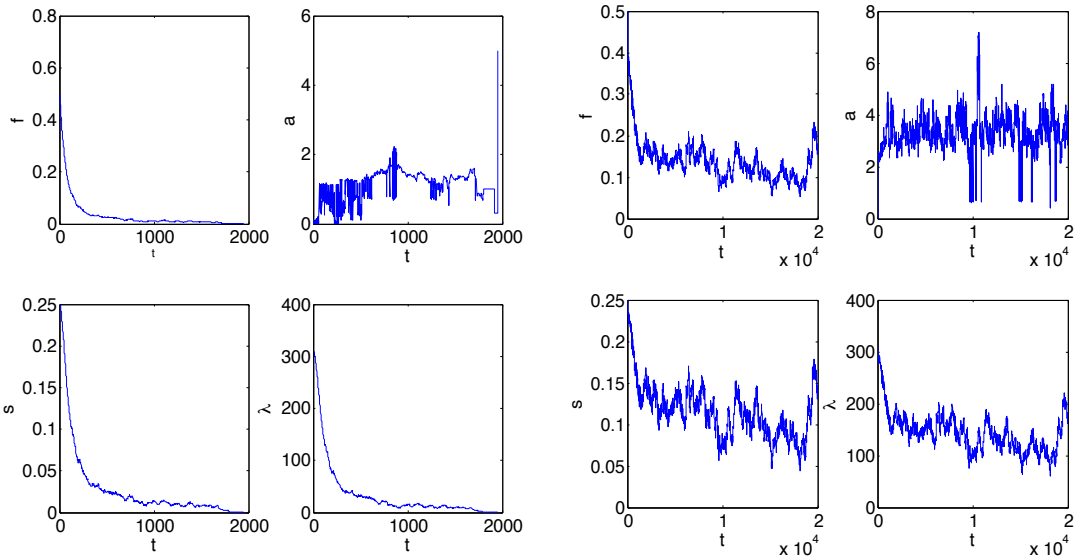

(a) A realization of time series for Fermi rule with $\sigma = 3$ and $b = 1.75$

(b) A realization of time series for Replicator rule with $\sigma = 1$ and $b = 1.50$

Figure 2.3 Realizations of time series obtained from spatial simulations: Frequency (f), Range (a), Sill (s) and Eigenvalue (λ).

Figure 2.3 shows the change of time series for mean, range, sill and the largest eigenvalue of the covariance matrix for some of the above defined discrete set of parameters. These parameters give information about the first and second moments of the spatial Markov chain. For example, in spatial PD game, cooperators form clusters. Here, the process a_t describes the size of the clusters. For the values of σ and b below the reverse diagonal, we see that density of the cooperators converges to zero. Thus these results show that the Markov chain converges in $2N \times 10^4$ time steps at most.

2.4.2 Simulations with Gaussian and Uniform Measures

In this section, simulations of Markov chains, described by the update rules, are used to show the frequency of cooperators for discrete, uniform and Gaussian kernels for PD game. On one hand, discrete Normal distribution determines distance based weights on the grid. In other words, discrete Gaussian structure determines the weights as a decreasing function of distances between cells on the lattice. The weights are controlled with the variance of the kernel σ. On the other hand, uniform distribution on a neighborhood with radius r gives equal weights to all cells in the neighborhood. The radius r is the parameter ruling out the size of the neighborhood in the case of discrete uniform distribution. On the contrary, the parameter σ is not only a

metric of the neighborhood size but also a metric ruling out the diffusion. This is to say it describes how strong interactions are in the neighborhood.

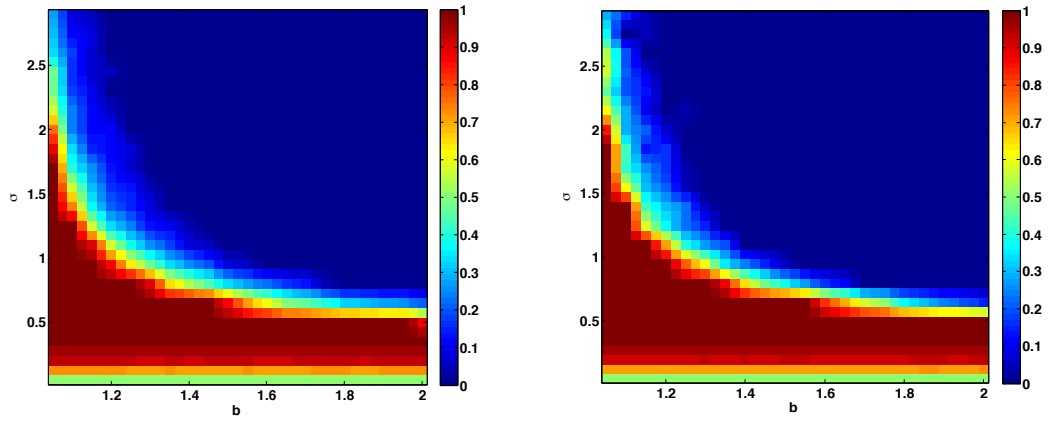

(a) Frequency of cooperators as a function of game parameter b and the kernel variance σ for Fermi rule

(b) Frequency of cooperators as a function of game parameter b and the kernel variance σ for Replicator rule

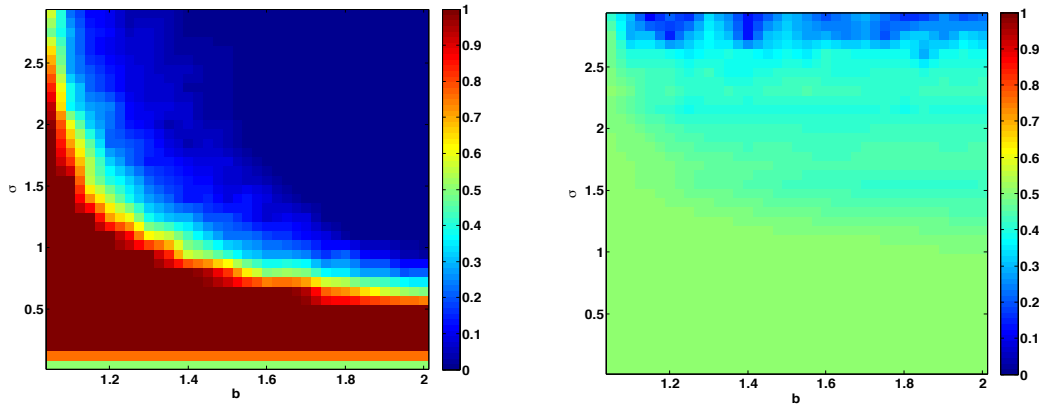

(c) Frequency of cooperators as a function of game parameter b and the kernel variance σ for Moran rule

(d) Frequency of cooperators as a function of game parameter b and the kernel variance σ for Best Take Over rule

Figure 2.4 Frequencies of cooperators in $\sigma - b$ plane

Figure 2.4 shows results obtained for frequency of cooperators in the population for the update rules, Fermi, Replicator, Moran and Best Take Over rules for random well mixed initial configuration using Gaussian neighborhood. Effect of the weights described by the parameter σ shows itself in the case of very small values. It can be seen that the dynamic is freezing for all rules in this case because the players do not interact with others in the neighborhood due to non-uniform weights. It can also be seen that there is no significant difference between two pairwise comparison rules, Fermi and replicator, while Moran rule supports cooperators in a larger parameter region in $b - \sigma$ plane. However, best-take over rule shows completely different

dynamical behavior due to deterministic nature of the rule and the spatial structure. Since interaction weight of each cell with itself is larger than any other ones in Gaussian neighborhood, it is unlikely to have larger weighted payoff for neighboring cells. These results are justified in the next subsection using the statistical method ANOVA.

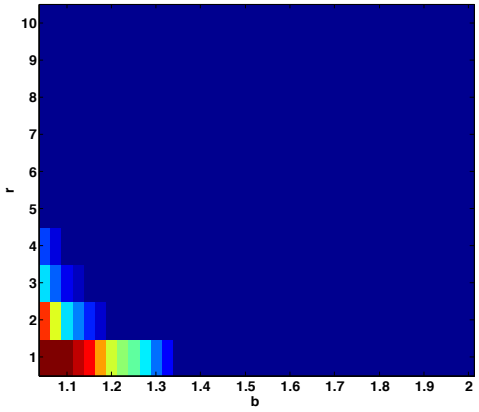

(a) Frequency of cooperators as a function of game parameter b and radius of Moore neighborhood r for Fermi rule.

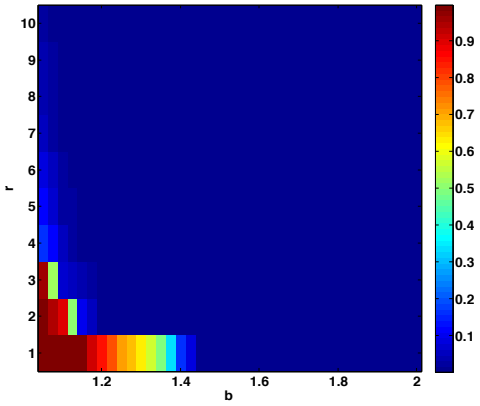

(b) Frequency of cooperators as a function of game parameter b and radius of Moore neighborhood r for replicator Rule rule

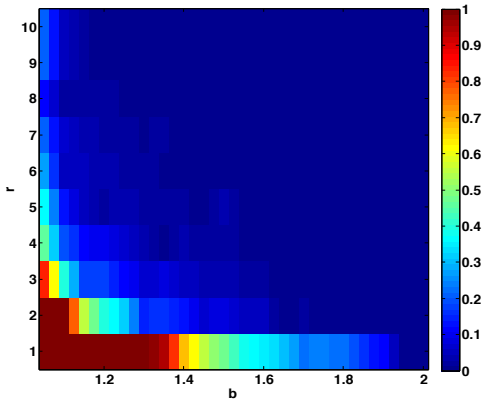

(c) Frequency of cooperators as a function of game parameter b and radius of Moore neighborhood r for Moran rule

Figure 2.5 Simulations with uniform measure

All three stochastic update rules are simulated in the case of classical Moore neighborhood with increasing values of radius r (see Figure 2.5). We consider the radius values $r = 1, 2, ..., 10$, since our simulations shows that frequency of cooperators is zero for pairwise comparison rules in the case of $r < 10$. Note that a similar study by Outsuki et al. [39] determines the average number of interaction size on graphs for the existence of cooperators in the case of small selection parameter. Our main purpose is to show the difference between two kernels in the case of

enlarging neighborhoods; one with uniform and the other with Gaussian weights. As seen from Figure 2.5, there is no freezing dynamics for Moore neighborhood supports less cooperation for all three stochastic rules with uniform interactions. However, the comparison of three rules in the case of uniform interactions is the same; there is a small difference between two pairwise comparison rules, Fermi and replicator, while Moran rule supports more cooperators in $r - b$ plane.

2.4.3 Effects of microscopic update rules

As discussed above, the microscopic update rules govern the dynamics of ESG models. However, discrepancies across different update rules exist as shown by the above simulation results (see Figure 2.4 and 2.5). This naturally rises the question whether the microscopic updates rules are significantly different for the purpose of capturing the game equilibriums accurately. We adapt statistical methods to investigate the repeated numerical simulations as computer experiments. ANOVA (Analysis of Variance) based on a suitable design of those computer experiment provides a reliable result for comparison of microscopic update rules.

Intuitively, the best take over rule (BTO) is a sort of deterministic greedy algorithm, which is expected to differ from the stochastic update rules. On the other hand, BTO is a limiting scheme of the Moran rule as discussed above. This implies that the Moran rule may possess potential deviations from replicator rule and Fermi rule.

The four microscopic update rules, from the point of view of experimental design, are treatments operating on the experimental unit which is the initial spatial configurations $D_0(\{0,1\}^{|\Omega|})$ for each individual based spatial-temporal process. To account the variability of the experiment as much as possible, Latin square was applied to propose meaningful blocks for the experiments. For a two players PD game, the parameter b and the standard deviation/dispersal ability σ define sensible blocks such that varying b from small to large corresponds to nature of the game in which the defectors vary from mild to aggressive, and varying σ from small to large corresponds to defectors with low mobility to high mobility. In short, effects of b and σ characterize the nature of the game and their contributions to the variability of game equilibriums should be accounted by blocking the experiments according to them.

To define a sensible computer experiment, it is necessary to record the responses of the simulations that can reflect the nature of games. Hence, we recorded meaningful statistics of the process after long run for individual simulation on fixed σ and b. As discussed before, the

equilibrium frequency, that captures the mean of the process and the largest eigenvalue of the sample covariance matrix from the last 1250 time points, that estimates the dependent structure are sensible statistics representing the game equilibrium and therefore the game nature. Those two responses essentially give the first and second moments of the temporal-spatial process defined by a ESG model. Hence, the computer experiment to be conducted can be summarized in the following statistical model:

$$\mathbf{Y}_{ijkl} = \boldsymbol{\mu_k} + \sigma_i + b_j + \boldsymbol{\epsilon_{ijl}} \tag{2.4.1}$$

for $k = 1, 2, 3, 4$, $i = 1, 2, 3, 4$ and $j = 1, 2, 3, 4$, where $\boldsymbol{\mu_k} = (\mu_k^1, \mu_k^2)^T$ represent the microscopic update rules' effects on equilibrium frequency mean and largest eigenvalue of the sample covariance matrix from the last 1250 time points $\mathbf{Y}_{ijkl} = (Y_{ijkl}^1, Y_{ijkl}^2)^T$, σ_i and b_j represent the effects of the nature of the games on its own equilibrium while ϵ_{ijl} stands for the variation due to the initial configuration and stochastic simulations. l is the number of simulation conducted for each experiment with certain update rules and pre-defined blocking choices for the game's nature. Statistical model (2.4.1) or the computer experimental design aims to quantify whether certain update rules are significantly different in terms of the game equilibrium distribution after accounting the possible effects from the pre-specified game's nature via σ and b.

The parameter region $\sigma < 1$ is not interesting as all stochastic update rules merge with each other according to Figure 2.4. We focus on the case $\sigma \in (1, 3)$ and $b \in (1, 2)$ for which coexistence equilibriums can be observed from one round of simulation. Parameter values $b = \{1.15, 1.40, 1.65, 1.90\}$ and $\sigma = \{1.30, 1.80, 2.30, 2.80\}$ are considered for blocks in the experiments. Four microscopic update rules are assigned within blocks based on Latin square design with suitable random initialization. The resulting design is shown in Table 2.1. To

$\sigma \setminus b$	1.15	1.40	1.65	1.90
1.30	BTO	R	F	M
1.80	R	F	M	BTO
2.30	F	M	BTO	R
2.80	M	BTO	R	F

Table 2.1 Latin square design of experiment

study how these microscopic update rules differ from each other, we conduct 48 computer experiments, i.e. 3 runs for each of the above 16 combinations. The experimental unites are 50×50 lattice with initial distribution being well mixed with sample mean equal to 0.5. The

whole data set therefore consists of 48 by 2 responses. At the iteration of $50^2 \times 10^4$, we perform statistical test for the two defined responses separately for simplicity (they are not independent however) based on the ANOVA, for which the results are shown in Table 2.2.

Effects of update rules	p-values for frequency	p-value for eigenvalue
BTO differs from Moran	$< 2 \times 10^{-16}$	$< 2 \times 10^{-16}$
BTO differs from Fermi	$< 2 \times 10^{-16}$	$< 2 \times 10^{-16}$
BTO differs from Replicator	$< 2 \times 10^{-16}$	$< 2 \times 10^{-16}$
Moran differs from Replicator	0.00284	0.006856
Moran differs from Fermi	0.002535	0.003995
Fermi differs from Replicator	0.967	0.8384

Table 2.2 Comparisons across four update rules based on computer experiments by the Latin square design

Based on the results in Table 2.2, we conclude that there is a statistically significant difference between the best take over rule and other three microscopic update rules (p-value $\ll 0.0001$); Moran rule is somehow different from Fermi and replicator rules (p-value $\ll 0.01$); and Fermi and replicator rules do not demonstrate any statistically significant difference. They define the same stochastic process and target on the same equilibrium in terms of frequency and distribution.

2.4.4 Effects of initialization on the game

This subsection is devoted to effect of initial configuration on long run frequencies of stochastic game dynamics. We considered only Fermi rule simulations for PD game using different initial conditions. We used well-separating and invasion models presented in Figure 2.1. For the well-separating model initial frequency of cooperators is taken as 0.46 and the long run behavior of the dynamics is given in Figure 2.6 (c). Figure 2.6 (a) represents the invasion model with small islands of cooperators and (b) represents the small island of defectors. Also note that these results are comparable to Figure 2.4 (a) which is the well mixed model given in Figure 2.1.

For sufficiently large values of σ, long-run behaviors the dynamics is similar for different initial configurations including the well-mixed model. The only difference appears in these simulations for small values of σ. As mentioned earlier, the dynamics is freezing in this case; individuals at a site does not capable of interacting with individuals at other sites due to weights dictated by the Gaussian kernel.

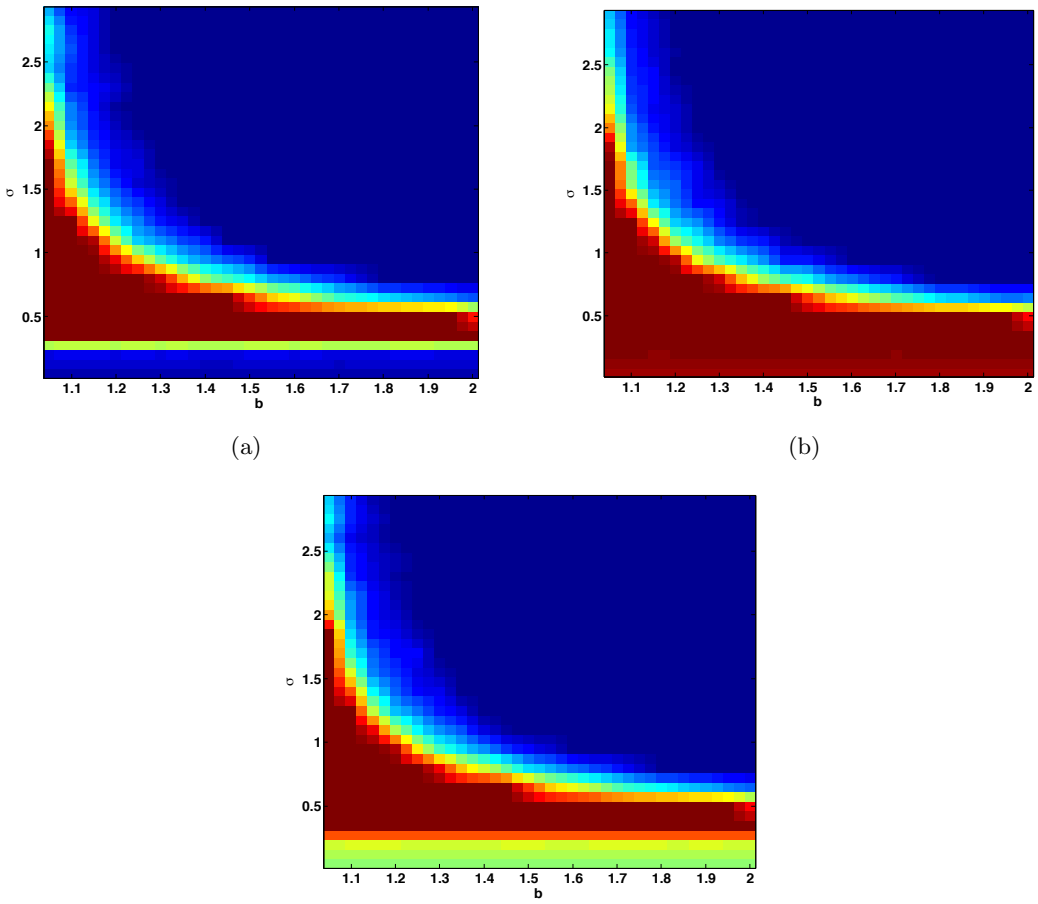

(a) (b)

(c)

Figure 2.6 Simulations of Fermi rule with initial configurations a) small island of defectors, b) small island of cooperators, c) well-seperated. See figure 2.1

We conclude that the initial configuration does not effect the long run behavior in the case of PD game for Fermi rule. By similarity of replicator and Fermi rules, it is expected that this result is also valid for replicator rule as well. Effect of initial configurations can also be studied for other two rules.

2.5 S-T Plane Simulations

In this section, we consider all four biologically important games in the parameter space described in section 2.2. Existing studies use $S-T$ plane simulations to compare the frequencies of cooperators/defectors for dynamics with different inputs such as different update rules [45], effect of asynchronism/synchronism [14] or underlying spatial structure (graphs vs regular lattices) with constant number of neighboring cell assumption [45, 14] in $S-T$ plane. Effect of

initial condition for all four games has been studied via simulations with small neighborhood assumption [45]. Moreover, behavior of deterministic dynamics of BTO rule with synchronous updates gives rise to chaotic behavior and under symmetry condition , Nowak and May reported existence of evolutionary kaleidoscopes [35, 36]. In short, the usage of these simulations are mainly used to show the difference between long run behavior of different inputs.

On the contrary, we consider $S-T$ plane simulations to study the effect of interaction strength and show convergence to mean field equations. Diffusion in the case of regular lattices and uniform interactions can be seen as neighborhood size whose effect has been studied in [24] for continuous PD game. The first study considering simulations with different neighborhood sizes/types via simulations on regular lattices is by Hauert [16]. A more general problem; effect of the average number of neighbors in a graph on cooperator frequency, is studied in [39]. The results leads us to cost to benefit ratio for small selection parameter.

A similar question can be asked for our model; how does the variance of dispersal kernel affect the equilibrium of the game? We answered this question for Fermi (replicator) rule using simulations by changing the variance of the kernel which is the major parameter that rule out the interaction strengths for individuals and the neighborhood size. Thus, in this section, our game is governed by three parameters two of which, T and S, are game parameters and the third one is the variance of the gaussian σ ruling out the interaction strength and neighborhood size. $S-T$ plane simulations are performed for different values of σ and it is conjectured that spatial dynamics of the game converges to mean field equation as σ gets larger. This result is expected since a Gaussian with very large σ and the support of whole lattice give uniform distribution on the neighborhood containing all individuals. Thus, as sigma gets larger, the effect of the spatial structure vanishes. We used the same simulation settings described in the previous section.

2.5.1 Simulation Results

First, we consider the proportion of the game parameters for which we have coexistence i.e. Snow-Drift game. Stability results for replicator dynamics in the next subsection shows that the coexistence region in the parameter space can be given explicitly by $1 > T > 0$ and $0 > S > -1$. The proportion of the parameters satisfying this inequalities is one fourth of the whole $S-T$ plane. Thus we consider proportion of coexistence region for spatial simulations as a function of σ. From the Figure 2.7, it is clear that the proportion of coexisting games

in the parameter space converges to one fourth which is the proportion of snow-drift game parameters.

The above result can be extended to be more informative by comparing frequencies of spatial simulations and the stable rest point of replicator equation for each S and T values. This will give us a geometric convergence in parameter space. Figure 2.7 shows frequencies of cooperators as a function of parameters S and T with six different σ values in the left column and the difference between spatial dynamics and the mean field dynamics in the right. As seen from the color maps that describe the differences between frequencies of cooperators in these two dynamics, As σ gets larger, the difference is smaller. Thus, it is clear that the spatial structure vanishes as sigma gets larger and the spatial dynamics gets closer to the mean field case asymptotically in the case of finite but large population. Thus, we conjecture that the spatial frequencies geometrically converge to the rest points of replicator equation in the parameter region $-1 < S < 1$, $0 < T < 2$. This result can be expressed by the following conjecture:

Conjecture 2.5.1. *The parameter level set of coexistence for two player ESG with fixed σ, A_σ where σ is as defined in information kernel K and microscopic update rules, is*

$$A_\sigma := \Big\{(S,T) \in (-1,1)\times(0,2) \mid \lim_{n\to\infty} \frac{1}{N^2}\sum_{i,j=1}^{N} I\{Z(i,j,n,S,T)_\sigma = 1\} \in (0,1)\Big\}$$

where $\frac{1}{N^2}\sum_{i,j=1}^{N} I\{Z(i,j,n,S,T)_\sigma = 1\}$ is the empirical measure of process $\{\boldsymbol{Z}_n^{S,T}\}$ defined by ESG at each generation n conditional on the fixed parameter (S,T) and σ. If the transition kernel for the process $\{\boldsymbol{Z}_n^{S,T}\}$ is defined by the pairwise comparison microscopic update rules as before, then

$$(1)\ \lim_{\sigma\to\infty} \mu(A_\sigma) = \mu(A) \quad \textit{(weak convergence)}$$

$$(2)\ \lim_{\sigma\to\infty} \mu(A_\sigma \Delta A) = 0 \quad \textit{(strong convergence)}$$

where A is the parameter level set of coexistence for mean field model with same payoff matrix defined by S,T, and μ is the Lebesque measure.

2.5.2 Large populations and proof of conjecture 2.5.1

Stochastic dynamics of well mixed population is studied in the case of finite population by Benaim and Weibull [5], and this process has fluid limits in the case of large population

assumptions [5, 53]. As we know, the mean field equation of the replicator rule is replicator equation [5]. We compared the stable rest points of this equation and the frequency of cooperators in the case of spatial simulations for increasing values of σ. Rest points and the stability of them is given by following discussion:

Stability of ODE: Without loss of generality take $R-T=1-T=a$, $P-S=-S=b$. The replicator equation reads as

$$\dot{x} = x(1-x)((a+b)x-b).$$

Equilibrium points of this equation are given by $x_1=0$, $x_2=1$ and $x_3=\frac{b}{a+b}$ if $\frac{b}{a+b}$ is positive. If $1>a>0$ and $1>b>0$, we have x_3 as an equilibrium point. $(a+b)x_0-b>0$ if $x_0>\frac{b}{a+b}$ and $(a+b)x_0-b<0$ if $x_0<\frac{b}{a+b}$. Thus, x_3 is not stable in this parameter region and the other two equilibriums are stable. This region corresponds to Stag-Hunt game.

If $0>a>-1$ and $0>b>-1$, we have the third equilibrium again and $(a+b)x_0-b<0$ if $x_0>\frac{b}{a+b}$ and $(a+b)x_0-b>0$ if $x_0<\frac{b}{a+b}$. This region corresponds to the Snow Drift Game.

In the case of other two regions, there is no third equilibrium. If $0>a>-1$ and $1>b>0$ ($1>a>0$ and $0>b>-1$), $(a+b)x_0-b<0$ ($(a+b)x_0-b>0$) respectively, since $0<x_0<1$. Thus, x_1 (x_2) is stable in this case and the region corresponds to the Prisoner's dilemma (Harmony) game.

Similar results has been obtained for grid populations with non-local interactions in [23] and chapter 3. The non-local replicator equation with periodic boundary conditions is given by

$$u_t(x,t) = J^\sigma * u - u + (u + J^\sigma * u - 2uJ^\sigma * u)((a+b)J^\sigma * u - b) \tag{2.5.1}$$

where w $J^\sigma * u = \int_{\mathbb{R}} J^\sigma(\|x-y\|)u(y,t)\,dy$. Suppose the kernel has support Ω and J^σ approaches uniform distribution $\frac{1}{|\Omega|}$ as $\sigma\to\infty$. The quantity measured in the simulations is the frequency of cooperators in the spatial domain that will be given by $p(t)=\frac{1}{|\Omega|}\int_\Omega u(x,t)\,dx$ Passing the limit as $\sigma\to\infty$ in equation (2.5.1) gives

$$\int_\Omega u_t(x,t) = u - p(t) + (u + p(t) - 2up(t))((a+b)p(t)-b)$$

By integrating the equation (2.5.1) in the spatial variable x, we get

$$\int_\Omega u_t(x,t) = \int_\Omega \big(u - p(t) + (u + p(t) - 2up(t))((a+b)p(t)-b)\big)\,dx$$

Thus, we obtain replicator ODE stability analysis of which is given above. This implies the conjecture is true for large population asymptotics.

2.6 Discussion and Future Work

This paper investigates the effect of non-local interactions on 2-player symmetric spatial games with a particular emphasis on PD game. Classical evolutionary game theory assumes random imitation, and classical cellular automata simulations consider local uniform interactions in a neighborhood. Both of these assumptions can be generalized to distance dependent weights. In the first case, we have a complete graph with uniform weights and in the second the spatial structure is given by a discrete uniform weight with the assumption that an individual interacts with a small set of the population. We consider weights as decreasing functions of distance which is biologically more realistic.

PD-game related results show that Moran rule supports more cooperation. This is also true for classical cellular automata simulations. In addition, the other generalized proportional update rule BTO differs from Moran rule and two other pairwise comparison rules. This is mainly due to the deterministic nature of the rule. Fermi and replicator rules give similar asymptotic frequencies. ANOVA results also show these two rules are not significantly different from each other. According to the effect of initial conditions for stochastic rules, the initial condition does not effect the general picture. The only exception is the case in which the deviation of the kernel is very small. In other words, if the kernel dictates very small or no interaction between grid points, the individual at a specific location interact only by itself and has no chance to imitate other strategies.

$S - T$ plane simulations compare asymptotic frequencies of Fermi rule with those of mean field dynamics. Similar to the case of classical cellular automata simulations, as the variance of the kernel, i.e. diffusibility of the individuals on the grid increases, the asymptotic frequencies of stochastic dynamics gets closer to the stable rest points of the mean field ODE. This result is proved using the mesoscopic limit of replicator rule.

We considered the spatial dynamics including the self interaction. A biological justification for the self interaction is given in [38, 35, 17]. It is also possible and computationally easy to consider stochastic dynamics excluding the self interaction. However, it is not possible to simulate Generalized proportional update rules using non self-interacting kernels. Thus further modifications are needed to define these rules properly. For example, we can use two different kernels one of which is self-interacting while the other is not. The former will be used to define update rules, the later is for payoff calculation, Some simulation results in [35] were obtained

by using both self-interacting and non self-interacting uniform distribution on a neighborhood.

It is also possible to simulate the dynamics in the case of synchronous updates. As studied in [14], effect of asynchronism on asymptotic frequencies of non-local spatial models can also be studied. Another possibility is to consider BTO in the case of synchronous updates. Clearly, it will be a completely deterministic update rule. Thus, chaotic behavior for this update rule and emergence of evolutionary kaleidoscopes can also be studied in the case of symmetric kernels, see for example Nowak [37]. In addition, effect of initial conditions can be investigated for synchronous and asynchronous rules. Especially synchronous BTO rule has a potential to exhibit very complex behavior under different initial conditions. Lastly, different kernels will lead to different asymptotic behaviors. It is possible to work with specific asymmetric or symmetric kernels.

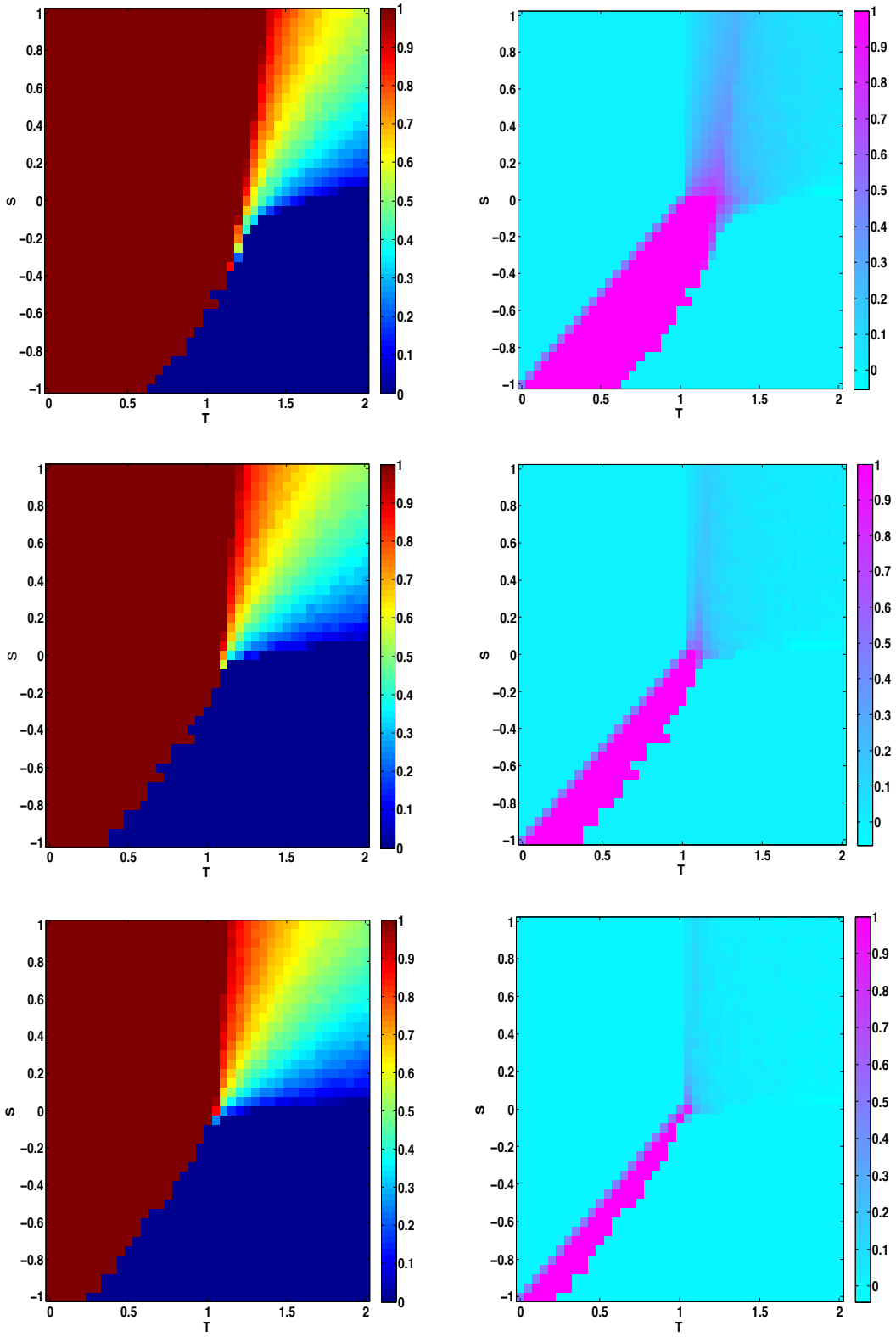

Figure 2.7 Fermi rule simulations in S-T plane. Sigma values changes top to bottom: $\sigma = 1, 1.5, 2, 2.5, 3, 3.5$. Left Column shows frequency of cooperators and right one shows the difference between left column and stable rest points of replicator equation.

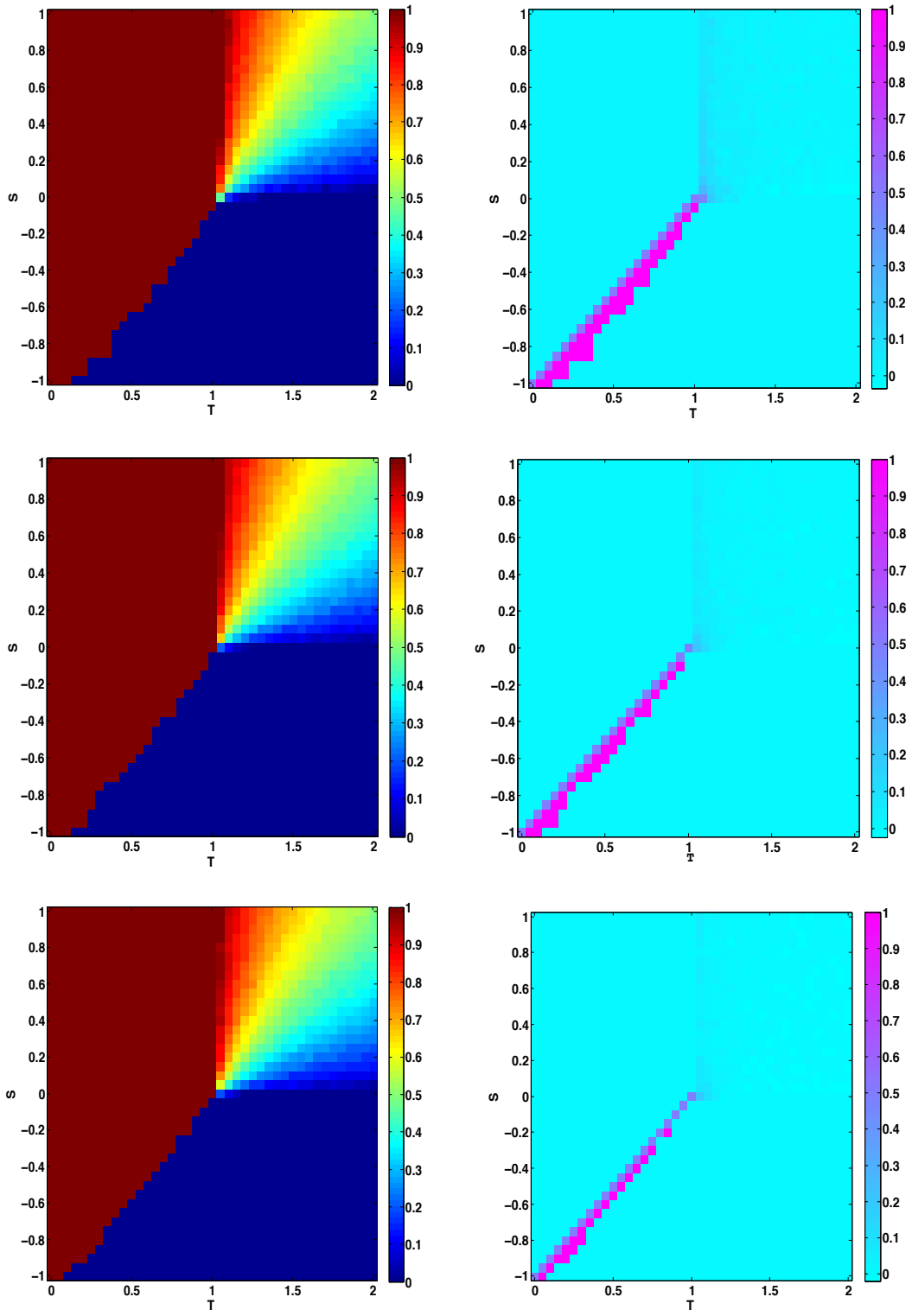

Figure 2.7 (continued)

CHAPTER 3. NON-LOCAL REPLICATOR EQUATION: TRAVELING WAVES AND SPREADING SPEEDS

3.1 Introduction

Evolutionary game theory is a basic tool to model emergence and maintenance of cooperation in biological and social communities. In a population consisting of cooperative and defective individuals, cooperators take a cost to assist others, while defectors choose more rational strategies to maximize one's own payoff. Thus, cooperation is expected to be rare in the population. However, cooperation is necessary for major evolutionary transitions in majority of complex ecosystems, evolution of chromosomes or transition from uni-cellular to multi-cellular organisms [50]. Game theoretical models provide a systematic way to study and explore this phenomena. Game theoretical framework models the interactions between individuals playing different strategies, by a payoff matrix $M = (m_{i,j})_{n\times n}$ and density dependent selection. In the literature, this interaction is modeled primarily by two games, Prisoner's Dilemma (PD) and Snowdrift (SD) [4].

In this chapter, we focus on the PD game in which players can make a decision to be cooperator (C) or defector (D). In the model, cooperation results in a benefit to the opposing player but defection produces neither cost nor benefit. Thus, fitness of defectors larger than the cooperators', implying defection is only Nash equilibrium. Evolutionary stable strategy (ESS) is a strategy that cannot be invaded by another strategy which is initially rare [4]. In a PD game, the only ESS is D. Evolutionary game theory converts these game theoretic concepts to the point of view of dynamical systems. Many game dynamics have developed lately, among which the replicator equation is the most favorable model [20]. The connection between Nash equilibrium of games and the stable equilibrium of the system is well established [20]. For PD game, cooperators go extinct, i.e its proportion converges to 0 asymptotically for any initial condition in $(0, 1)$. Moreover, replicator equation and other equations can be obtained as deterministic limits of stochastic birth and death processes [5]. Hence, stochastic

dynamics can be tracked by the deterministic one under large population assumption.

Stochasticity itself is not enough to establish persistence of cooperators in a PD game because of the asymptotical behavior of its deterministic limiting ODE. In literature, three approaches exist to overcome this difficulty. The first one is the replicator diffusion equations. This dynamic approach considers mobil individuals, modeled by diffusion, with same or different diffusion rates [21, 18, 19]. Existence of traveling waves in spatially distributed moving individuals implies invasion of a defector population by cooperators. The second approach is to use Markovian cellular automata simulations for populations on grids. Individuals do not move but collect their payoffs from a small spatial neighborhood. Simulation results also give rise to persistence of cooperators in a PD game for example see [38] and references therein. The last approach is to use non-Markovian dynamics. It considers a spatial or well-mixed population of individuals with memory. In this approach, history of strategies played by each player is saved and affects the probability of choosing a strategy of another player [41].

We consider a grid population described in [55] with nonlocal interactions. Spatial weights on the grid are described via discrete kernels. Using the theory developed in [23] and modifying the rate function given in [53], we construct non-local replicator equations directly from microscopic rules. Resulting integro-differential equation is the deterministic limit of stochastic grid population which describes the spatial and temporal dynamics of individuals playing an n strategy game in general.

In this study, we focus on the asymptotic behavior of this equation for the PD game, and ask what the asymptotic tendency of spread of defectors is. The questions involving spread and invasion are naturally connected to mathematical theories: traveling waves and asymptotic speed of spread (hereafter spreading speed). Traveling waves theory is a well known concept in ecology. Existence of monotone waves implies non-invasibility of cooperators. Existence of such waves in the case of mobile players has been extensively studied [21, 19]. Spreading speed was introduced for reaction-diffusion equations in [3] and further it has been applied to a non-local epidemic model [2] which describes the long term behavior of the population in spatial habitats. Since then it has been applied to many ecological and epidemic models, for example see [25, 54].

This chapter is organized as following. In section 3.2, we first give a short description of the stochastic model and its mesoscopic limits. Then we introduce the modified rate function and obtain system of non-local replicator equations. In addition, a single equation is derived

for two strategy games and its parameter region is investigated in terms of quasi-monotonicty, linear determinacy, monostability and bistability. In section 3.3, existence and non-existence of traveling wave solutions are established in a parameter region where the non-local equation is quasi-monotone and linear determinant. In addition, we consider spreading speeds without linear determinacy condition. It is shown that there exists a unique spread speed and it is equal to traveling wave speed if linear determinacy condition is satisfied. In section 3.4, we give technical details of the methods used and proofs of theorems.

3.2 Model derivation

In this section, we present the general spatial stochastic process and its deterministic limit that has the form of an integro-differential equation. Modifying the transition probabilities for a non-spatial birth-death process given in [53] gives non-local replicator equations. We then state the equation for two player games and give some basic properties of the equation.

3.2.1 Stochastic model and Mesoscopic limit

Before stating the limiting integro-differential equations, we recall the underlying stochastic process on a domain of grid Λ, a subset of Z^d. Suppose individuals are located at the sites of Λ. The interaction strength between individuals at different sites is given by a discrete kernel $\mathcal{J}(\acute{x}-\acute{y})$ satisfying $\sum_{\acute{x}}\mathcal{J}(\acute{x})=1$. They collect their payoffs from the sites according to the weight assigned by the kernel and the payoff matrix $M=[m_{ij}]$. At a fixed time t suppose the configuration of the lattice is given by β, and $\beta(\acute{x})$ denotes the strategy played by the individual at site $\acute{x}$. The payoff of the individual with strategy i at site $\acute{x}$ is given by

$$p(\acute{x},\beta,i)=\sum_{\acute{y}\in\Lambda}\mathcal{J}(\acute{x}-\acute{y})m_{i\beta(\acute{y})}$$

We assume that each agent has a exponential alarm clock with rate 1 and s/he updates his/her strategy to i when the configuration is β according to a rate function $r(\acute{x},\beta,i)$ where $\acute{x}\in\Lambda$ is the spatial location. This model was proposed in [55] and defined in terms of its Markov generator in [23] (see also section 3.4.1). Cellular automata simulations with small neighborhood assumption have been studied by many authors (see for example [36, 35]). Individual based simulations of this model with Gaussian kernels is considered in the second chapter of this thesis.

There are several different rate functions presented in [23]. However, we consider rate functions of the form

$$r(\acute{x},\beta,i)=\omega(\acute{x},\beta,i)\big[F(p(\acute{x},\beta,i)-p(\acute{x},\beta,\beta(\acute{x})))\big] \tag{3.2.1}$$

where $\omega(\acute{x},\beta,i)=\sum_{\acute{y}\in\Lambda}\mathcal{J}(\acute{x}-\acute{y})\delta(\beta(\acute{y}),i)$ which is the probability of finding individuals playing strategy i in the neighborhood of $\acute{x}$ with respect to measure $\mathcal{J}$. We use this form because the rate functions used to obtain replicator equations have this form. For example, the classical rate function to obtain replicator equations [20, 5] is given by

$$\omega(\acute{x},\beta,k)\big[p(\acute{x},\beta,k)-p(\acute{x},\beta,\beta(\acute{x}))\big]_+ \tag{3.2.2}$$

where $[s]_+=\max\{0,s\}$.

We now introduce the space scaling. Suppose $J(x)$ is a non-negative and integrable function satisfying $\int_{\mathbb{R}^d}J(x)=1$. The continuous kernel is a result of mesoscopic scaling, which is closely related to the discrete kernel $\mathcal{J}$ see [23, 42]. The connection between the discrete kernel and J is given by $\mathcal{J}^\gamma(\acute{x}-\acute{y})=\gamma^d J(\gamma(\acute{x}-\acute{y}))$ here $\gamma^{-d}=n^d=|\Lambda|$. Note that $|\Lambda|$ is the size of the population in d dimensional integer lattice Λ.

Suppose $A\subset\mathbb{R}^d$ is the mesoscopic domain and $A^\gamma=\gamma^{-1}A\cap Z^d$ is the microscopic domain. Denote the density of agents with strategy i at $x\in\mathbb{R}^d$ by $u_i(x)$. Under this scaling, as $\gamma\to 0$ microscopic domain approaches the mesoscopic continuum, A and an individual at x interacts with an increasing number of agents.

It has been shown in [23] that the deterministic limit of this Markov chain is an integro-differential equation given by

$$\frac{\partial}{\partial t}u_i(x,t)=\sum_{k=1}^{n}r(x,k,i,\mathbf{u})u_k-u_i\sum_{k=1}^{n}r(x,i,k,\mathbf{u}). \tag{3.2.3}$$

where $r(x,k,i,\mathbf{u})$ is a real valued function describing the strategy change from k to i and $\mathbf{u}=(u_i(x,t))_{1\times n}$ is the the vector i^{th} component of which denotes the frequency of i^{th} strategist at spatial position $x\in\mathbb{R}^d$ and time $t\in\mathbb{R}^+$. The function $r(x,k,i,\mathbf{u})$ corresponding to the rate function (3.2.2) is given by

$$J*u_i(x,t)\big[\sum_{l=1}^{d}(m_{kl}-m_{il})J*u_l\big]_+$$

where $J*u_i=\int_{\mathbb{R}^d}J(x-y)u_i(y)\,dy$.

By using this rate function in (3.2.3), Hwang [22] obtained an integro-differential equation. However, even exploring the parameter space of this equation for basic properties such as quasi-mononicity or linear determinacy is a difficult task.

3.2.2 Non-local replicator equation

Equation (3.2.3) describes the time and space evolution of the different types of individuals/players that evolve according to the rate function c on the domain. Instead of using the rate function (3.2.2) to obtain non-local replicator equations, we use the following function obtained from transition probabilities given in [53]

$$r(x,i,k,\mathbf{u}) = J * u_k(1 + w\frac{\sum_{l=1}^{n}(m_{kl} - m_{il})J * u_l}{\Delta p}) \tag{3.2.4}$$

where Δp is the maximum payoff difference and w is the the intensity of selection restricted to $(0,1]$. The function given above has to be non-negative otherwise corresponding rate function takes negative values. Using the fact that $\sum_{i=1}^{n} u_i = 1$, and rescaling the parameters by $\Delta p = \max_{i,k,l} |m_{kl} - m_{il}|$, we get the restriction on the parameter space $\max_{i,k,l} |m_{kl} - m_{il}| \leq 1$ Employing (3.2.4) in (3.2.3) gives the non-local replicator equation

$$\frac{\partial}{\partial t}u_i = J * u_i - u_i + w[(J * u_i + u_i)\sum_{k=1}^{n} m_{il}J * u_l - \sum_{k,l=1}^{n} m_{kl}(u_k J * u_i + u_i J * u_k)J * u_l]. \tag{3.2.5}$$

We have the rate function with spatial effects dropped as

$$r(i,k,\rho) = \rho_k(1 + w\sum_{l=1}^{n}(m_{kl} - m_{il})\rho_l.$$

where m_{ij} are rescaled payoffs and ρ_k denotes the frequency of $k^{\mathbf{th}}$ strategist. Using this rate in the corollary 4 of [23] or taking $J = \delta$ gives the well-known replicator equation

$$\dot{\rho}_i = \frac{2w}{\Delta p}(\rho_i \sum_{k=1}^{n} m_{il}\rho_l - \sum_{k,l=1}^{n} m_{kl}\rho_i\rho_k\rho_l). \tag{3.2.6}$$

Here $J = \delta$ means that individuals at a spatial location do not interact with the other spatial locations. therefore we get a replicator equation at each spatial location. Equations (3.2.5) and (3.2.6) shares many common properties. For example any constant solution of (3.2.6) is also a space homogenous solution of (3.2.5) and vice versa [23]. Moreover, the dynamics depends only on the payoff differences as seen from the equation (3.2.5).

In section 3.4.1, we provide a technical discussion of the method introduced in [23] and we present necessary conditions on $r(\acute{x},\beta,i)$ and $r(x,i,k,\mathbf{u})$.

3.2.3 Two player games and one dimensional replicator equation

In this section, we present the equation for two player games along with the restrictions on the parameter space. We consider the payoff matrix

$$\begin{pmatrix} a_1 & a_2 \\ 0 & 0 \end{pmatrix},$$

where $|a_i| \leq 1$ for $i = 1, 2$. Using the fact $u_1 = 1 - u_2$ and the payoff matrix in equation (3.2.5), we obtain the following single equation:

$$\frac{\partial}{\partial t}u = H[u] := J * u - u + w(u + J * u - 2uJ * u)((a_1 - a_2)J * u + a_2) \tag{3.2.7}$$

where $a_1 = m_{11} - m_{21}$ and $a_2 = m_{12} - m_{22}$. Using the parameter regions for replicator equations we can classify this equation as

- Monostable: $u = 0$ (or 1) is stable equilibrium and there is no interior rest point if $a_1 < (>)0$ and $a_2 < (>)0$
- Bistable: there exists $c \in (0, 1)$ such that c is stable if $a_1 > 0$ and $a_2 < 0$.

We consider this equation in one space dimension with monostable nonlinearity. Note that the equation is obtained only for bounded regions with periodic and fixed boundary conditions in [23]. As noted in [42, 23] fixed boundary result can be extended to whole real numbers.

For the sake of simplicity, take $b = a_2$ and $a = a_1 - a_2$. We state our results for the parameter region $1 > a > -1$ and $1 > b > 0$. If we take $u(x, t)$ as the density of defectors at the spatial position x and time t then this single equation models the PD game.

Linearization (or Fréchet derivative) of $H[u]$ near 0 is given by

$$\mathcal{M}[u] = -(1 - wb)u + (1 + wb)J * u \tag{3.2.8}$$

We call an equation linearly determinate if it satisfies the following condition: for each positive ϵ there is a δ such that

$$H[u] \leq \mathcal{M}[u] \quad \text{and} \quad (1 - \delta)\mathcal{M}[u] \leq H[u] \tag{3.2.9}$$

when $0 \leq u \leq \epsilon$. It is called quasi-monotone if right hand side of the equation (3.2.7) is increasing function of $J * u$.

The non-local replicator equation (3.2.7) is neither quasi-monotone nor linearly determinate in whole parameter space. The equation is said to be quasi-monotone and linearly determinate, if the parameter region is restricted to

P1: $w(b-a) < 1$

P2: $a \leq 0$,

respectively. Condition **P1** is essential for the comparison principle and it naturally arises in the proof of theorem 3.3.2. this condition holds for sufficiently small selection parameter, w. thus it is biologically reasonable assumption. Before stating our assumptions on the

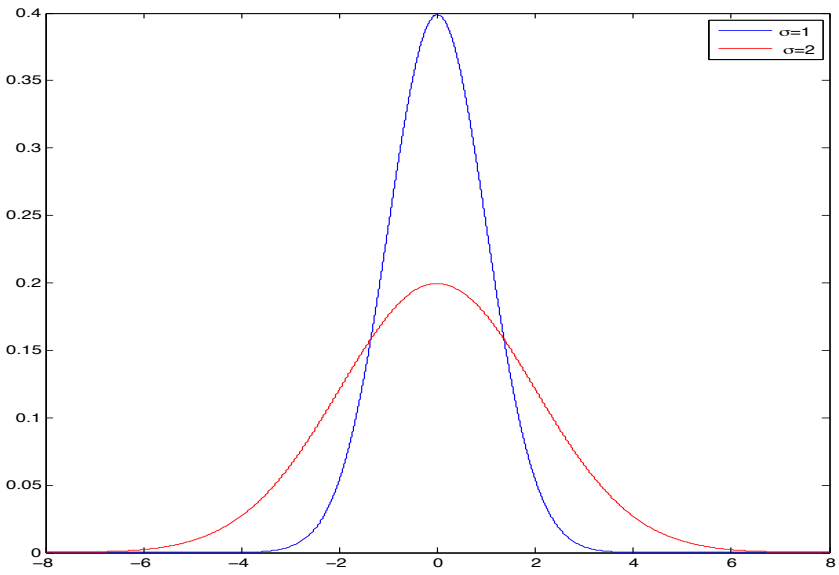

Figure 3.1 *p.d.f* of two Gaussian kernels.

interaction kernel J, define the moment generating function:

$$M(s) = \int_{\mathbb{R}} e^{su} J(u)\, du.$$

In this chapter, we assume J satisfies

J1: $J \geq 0$ and $\int_{\mathbb{R}} J(x)\, dx = 1$

J2: $M(s) < \infty$ whenever $s^- < s < s^+$ for some $s^- < 0$ and $s^+ > 0$

3.3 Analysis of the model

In this section, we consider the nonlocal replicator equation for parameters for which it is quasi-monotone. Using the comparison principle, we show that asymptotically cooperation is evolutionary stable if the traveling wave speed is sufficiently large or small. Otherwise, initially small population of defectors takes over the population.

3.3.1 Existence and Non-Existence of Traveling Waves

In the case of monostable nonlinearity, traveling waves implies defectors cannot invade the population of cooperators in either negative or positive direction. Existence of such solutions for evolutionary games with mobil individuals is given in [19, 21]. Here we derive the minimal speed of traveling wave using the linearized system. We use the theory developed in [46] to show the existence of traveling waves.

Following [33], we obtain the critical traveling wave speeds by using the linearization

$$\frac{\partial}{\partial t}u = \mathcal{M}[u]$$

and changing the coordinate frame to traveling wave coordinates $\xi = x + ct$ where c is speed of the traveling wave. Then we obtain,

$$cU(\xi) = -(1 - wb)U(\xi) + (1 + wb)\int_{\mathbb{R}} J(\xi - x)U(x)\,dx. \tag{3.3.1}$$

Using the exponential ansatz $U(z) = e^{-sz}$ in equation (3.3.1) we get the characteristic equation

$$\Delta_c^0(s) = -cs + (1 + wb)M(s) - (1 - wb).$$

It is clear that Δ_c^0 is convex and it takes negative values for sufficiently small (large) c and negative (positive) s. This implies existence of two zeros of Δ_c^0. In addition, it has double root for some $c_0^{\pm}$. Thus, we can derive the right and left traveling wave speeds by

$$\begin{aligned} c_0^+ &= \inf_{s>0} \frac{-(1 - wb) + (1 + wb)M(s)}{s} \\ c_0^- &= \sup_{s<0} \frac{-(1 - wb) + (1 + wb)M(s)}{s}, \end{aligned} \tag{3.3.2}$$

respectively. The traveling wave solution $u(x, t) = U(x + ct)$ of (3.2.7) satisfies the equation

$$cU' = J * U - U + w(U + J * U - 2UJ * U)(aJ * U + b) \tag{3.3.3}$$

with boundary conditions

$$U(-\infty) = 0 \text{ and } U(\infty) = 1 \quad \text{for} \quad c > c_0^+$$

and

$$U(-\infty) = 1 \text{ and } U(\infty) = 0 \quad \text{for} \quad c < c_0^-$$

Following theorem establishes the existence and non-existence of traveling wave solutions in terms of traveling wave speeds.

Theorem 3.3.1. *Suppose that J satisfies **J1-J2**, and **P1-P2** holds. Then a monotone solution U of (3.3.3) such that $0 \leq U \leq 1$ exists only for $c \notin (c_0^-, c_0^+)$.*

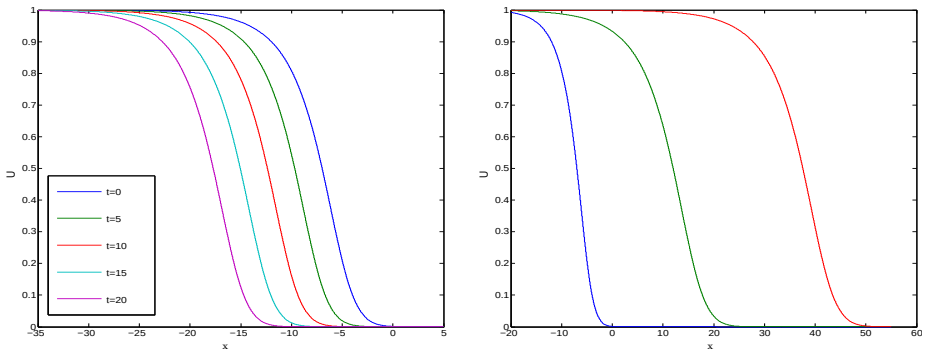

(a) Traveling wave solutions for $\sigma = 0.5$ (b) Non-existence of traveling wave solutions for $\sigma = 1$

Figure 3.2 Traveling waves. Waves were computed for the game with parameters $w = b = 0.5$, $a = -0.3$ and c=-0.65. Successive waves were separated by 5 time units. 40000−points were used in the spatial domain $[-100, 100]$ and the step size for spatial domain was 0.005. Time step was chosen as 0.0005. The Cauchy data was 1 on left half of the spatial domain and 0 on the right. (a) shows the existence and (b) shows non-existence of traveling waves of the game with the parameters given above.

Theorem 3.3.1 implies the existence of traveling waves, if the speed of the wave is outside of (c_0^-, c_0^+). One of the interesting questions is how the variance of the kernel effects the traveling wave speed. Simulations with symmetric truncated Gaussian kernel with two different variances show that the length of the interval (c_0^-, c_0^+) increases with σ, see Figure 3.2.

3.3.2 Asymptotic Speed of Propagation

In this section we define the asymptotic speed of propagation and show that this speed actually coincides with the traveling wave speed whenever linear determinacy condition is satisfied. In addition, asymptotic analysis of (3.2.7) enables us to show invasion of species in a larger set of parameters than that of traveling waves using the theory developed in [29]. Before defining the asymptotic speed we state the following theorem which gives the existence and uniqueness of solutions to equation(3.2.7) and the comparison principle.

Theorem 3.3.2. *Assume that J satisfies (**J1-2**). Then there exists a unique solution $u(x,t) \in BUC(\mathbb{R}\times\mathbb{R}^+)$ of (3.2.7) such that $0 \le u \le 1$. Moreover, suppose that (**P1**) holds and for $i = 1, 2$, u_i is the solution of (3.2.7) corresponding the initial datum $u_i(x,0) = u_{0i}$,*

$$\text{if} \quad 0 \le u_{01} \le u_{02} \le 1 \quad \text{then} \quad 0 \le u_1 \le u_2 \le 1$$

for all $(x,t) \in \mathbb{R}\times\mathbb{R}^+$

The condition **P1** is essential to prove comparison principle. The proof of above theorem is given in section 3.4.3,

Since it enables us to write equation (3.2.7) as an integral equation(see section 3.4.4), we introduce the operator $\mathbf{F}$ as

$$\mathbf{F}[u](x,t) = (1+bw)J*u - 2bwuJ*u + awJ*u(u + J*u + -2uJ*u),$$

then equation (3.2.7) can be written as

$$\frac{\partial}{\partial t}u(x,t) = -(1-bw)u(x,t) + \mathbf{F}[u](x,t), \tag{3.3.4}$$

From now on, we work with a coordinate frame which moves with speed c. For any $c > 0$ set $\xi = x + ct$. Thus, above equations can be written as

$$\frac{\partial}{\partial t}u(\xi,t) = Q_c[u(\xi,t)] \tag{3.3.5}$$

where $Q_c[u] = -cu_\xi - (1-bw)u + \mathbf{F}[u]$. The result of theorem 3.3.2 is also valid for (3.3.5), see proof in section 3.4.3.

The next lemma is an intermediate step necessary to define the spreading speed. It states that the solution of equation (3.3.5) with a positive initial value converges to 1 in the moving coordinates for $c \in (c_0^-, c_0^+)$.

Lemma 3.3.3. *Suppose that **J1-J2** and **P1** and $I \subset \mathbb{R}$ be an interval. Then the solution of the initial value problem*

$$\begin{aligned} \frac{\partial}{\partial t}u &= Q_c[u] \\ u(\xi,0) &\neq 0 \quad \textit{for} \quad \xi \in I \end{aligned}$$

satisfies $\lim_{t\to\infty} u(\xi,t) = 1$ *for* $c \in (c_0^-, c_0^+)$.

This lemma is proved using squeezing technique introduced by Aronson [2] and further developed in [30] in section 3.4.4.1.

Since our equation does not satisfies linear determinacy condition, super solution method [2, 31] does not work. However It is possible to define right and left spreading speeds as

$$\begin{aligned} c_*^+ &= \inf\{c \geq c_0^+ \,|\, \lim_{t\to\infty} u(x+ct,t) = 1\} \\ c_*^- &= \sup\{c \leq c_0^- \,|\, \lim_{t\to\infty} u(x+ct,t) = 1\} \end{aligned} \tag{3.3.6}$$

In section 3.4.5, we write the equation (3.2.7) as a recursion and show that definition of spreading speeds is valid.

The following theorem proved in section 3.4.5 gives the asymptotic behavior of the equation in terms of spreading speed c.

Theorem 3.3.4. *Suppose **J1-J2** and **P1** hold. If the initial data is compactly supported and* $0 \in (c_0^-, c_0^+)$ *then*

$$\lim_{t\to\infty} u(x+ct,t) = \begin{cases} 1 & \textit{if} \quad c \in (c_*^-, c_*^+) \\ 0 & \textit{if} \quad c \notin (c_*^-, c_*^+) \end{cases}$$

Moreover, if $a \leq 0$ *then* $c_0^\pm = c_*^\pm$.

Above theorem shows the relation between the traveling wave and the spreading speeds. If parameter a is negative, then these two speeds are the same and do not depend on the value of a. Otherwise, spreading speed is always greater than or equal to traveling wave speed. The effect of a is shown in Figure 3.3. Simulations with two different values of the parameter show that the spreading speed increases with a.

Here we would like to denote that the quasi-monotonicty condition, **P1** cannot be relaxed unless we assume extra conditions on both the kernel and initial conditions. To prove monotonicity, the condition guarantees the non-negativity of derivative of the right hand side of

equation (3.2.7) with respect to $J * u$, see proof of theorem 3.3.2. However, the right hand side takes its minimum value at $u = 1$ and $J * u = 0$. Thus, comparison principle in this case depends on both initial condition and the kernel.

3.4 Technical details and proofs

3.4.1 Mesoscopic limits

Let S denote the set of strategies. Consider β_t as the configuration of the lattice at time t. Suppose there is an exponential clock of each site and a chosen site $\acute{x}$ updates its strategy according to the configuration at time t. The generator of this Markov process is then given by

$$(Lg)(\beta) = \sum_{\acute{x}\in\Lambda}\sum_{k\in S} r(\acute{x},\beta,k)(g(\beta^{\acute{x},k}) - g(\beta)).$$

where $\beta^{\acute{x},k}(\acute{y}) = k$ if $\acute{y} = \acute{x}$ and it is $\beta(\acute{y})$ otherwise. ($\beta^{\acute{x},k}$ represents the configuration in which the agent at site $\acute{x}$ switches from his current strategy to a new strategy k.)

Suppose $A \subset \mathbb{R}$ is the mesoscopic domain and $A^\gamma = \gamma^{-1}A \cap Z^d$is the microscopic domain.

Definition 3.4.1. The empirical measure $\pi^\gamma : S^{A^\gamma} \to \mathbb{P}(A \times S)$ is given by

$$\pi^\gamma(\beta) = \frac{1}{|A^\gamma|}\sum_{\acute{x}\in A^\gamma} \delta_{(\gamma\acute{x},\beta(\acute{x}))}$$

where $\mathbb{P}(A \times S)$ denotes the set of all probability measures on $A \times S$.

Let β_t^γ be the stochastic process with generator

$$(L^\gamma g)(\beta) = \sum_{\acute{x}\in A^\gamma}\sum_{k\in S} r^\gamma(\acute{x},\beta,k)(g(\beta^{\acute{x},k}) - g(\beta))$$

Assumptions on strategy revision rate $r^\gamma(\acute{x},\beta,k)$ are that there exists a real valued function $r(x,i,k,\pi)$ where $x \in A$, $i,k \in S$ and $\pi \in \mathbb{P}(A \times S)$.

R1: $r(x,i,k,\pi)$ satisfies

$$\lim_{\gamma\to 0}\sup_{\acute{x}\in A^\gamma,\beta,k} |r^\gamma(\acute{x},\beta,k) - r(\gamma\acute{x},\beta(x),k,\pi^\gamma(\beta)| = 0$$

R2: $r(x,i,k,\pi)$ is uniformly bounded i.e there exist an $M > 0$ such that

$$\sup_{x\in A,i,k} |r(x,i,k,\pi| \le M$$

R3: $r(x,i,k,fm)$ satisfies Lipchitz condition with respect to x :

$$\sup_{x\in A,i,k} |r(x,i,k,u_1 m) - r(x,i,k,u_2 m)| \leq L||u_1 - u_2||_{L^1}$$

Here $m = dx \otimes di$ where dx is the Lebesque measure on A and di is the counting measure on S.

The next result connects the stochastic process with the integro-differential equation.

Theorem 3.4.2. *[23] Suppose the rate r satisfies **R1-3**. Let $\mathbf{u}$ be a $L^\infty(A\times S)$ function satisfying $0 \leq u_i \leq 1$ and $\sum_{i\in S} u_i = 1$ for all $x \in A$. In addition, assume that the initial distribution is a family of measures with slowly varying parameter associated to the profile of $\mathbf{u}$. Then for every $T > 0$*

$$\lim_{\gamma\to 0} \pi_t^\gamma(\beta_t) = \mathbf{u}(t,x)m \qquad \textit{in probability}$$

uniformly for $0 \leq t \leq T$ and u satisfies the following differential equation for $x \in A$, $i \in S$

$$\frac{\partial u_i}{\partial t}(x,t) = \sum_{k\in S} r(x,k,i,\mathbf{u})u_k(x,t) - u_i(x,t)\sum_{k\in S} r(x,i,k,\mathbf{u})$$

with initial condition $\mathbf{u}(x,0)$

The following result can be obtained from the above theorem directly. For the proof of this corrolary we refer to [5].

Corollary 3.4.3. *Suppose that the interaction is uniform with the same assumptions on the rate c. Assume there exists $\rho_0 \in \Delta$ such that the initial condition η_0^n satisfies*

$$\lim_{N\to\infty} \eta_0^N = \rho_{\mathbf{0}} \textit{ in probability}$$

then for every $T > 0$

$$\lim_{N\to\infty} \eta_t^N = \rho_i \textit{ in probability}$$

uniformly for $0 \leq t \leq T$ and f satisfies the following initial value problem:

$$\frac{d\rho_i}{dt} = \sum_{k\in S} r^N(k,i,\rho)\rho_k(u) - \rho_i(u)\sum_{k\in S} r^N(i,k,\rho)$$
$$\rho(0) = \rho_{0i},$$

where $c^N(k,i,\rho) = \rho_i(\sum_{l\in S} m_{il}\rho_l - \sum_{l\in S} m_{kl}\rho_l)$.

3.4.1.1 Replicator rule and replicator equations

The rate given by equation 3.2.1 satisfies above conditions **R1-3** if the function F satisfies global Lipschitz condition [22]. Thus, above theorem can be used to obtain replicator equations for $F(s) = 1 + \frac{s}{\Delta p}$. The corresponding function $r(x, i, k, \mathbf{u})$ with this rate is given by equation 3.2.4.

Corollary 3.4.4. *Suppose that there is no spatial structure then the rate with $F(s) = 1 + \frac{s}{\Delta p}$ gives the replicator equation.*

Proof. If there is no spatial structure then the rate function can be written as

$$r(i, k, \rho) = \rho_k[1 + w(\sum_l m_{kl}\rho_l - \sum_l m_{il}\rho_l)] \tag{3.4.1}$$

by taking $\mathbf{u}(x, t) = \rho$ and using the equality $J(x)dx = \frac{1}{|A|}$. Applying above corollary gives

$$\begin{aligned}
\frac{d\rho_i}{dt} &= \sum_{k\in S} r(k, i, \rho)\rho_k - \rho_i \sum_{k\in S} r(i, k, \rho) \\
&= \sum_{k\in S} \rho_i[1 + w(\sum_l m_{il}\rho_l - \sum_l m_{kl}\rho_l)]\rho_k - \rho_i \sum_{k\in S} \rho_k[1 + w(\sum_l m_{kl}\rho_l - \sum_l m_{il}\rho_l)] \\
&= \sum_{k\in S} \rho_i[1 - w(\sum_l m_{il}\rho_l - \sum_l m_{kl}\rho_l)]\rho_k - \rho_i\rho_k[1 + w(\sum_l m_{kl}\rho_l - \sum_l m_{il}\rho_l)] \\
&= 2w\rho_i \sum_{k\in S} \rho_k \sum_l m_{il}\rho_l - 2w\rho_i \sum_{k,l} m_{kl}\rho_l\rho_k) \\
&= 2w\Big(\rho_i \sum_l m_{il}\rho_l - \rho_i \sum_{k,l} m_{kl}\rho_l\rho_k\Big).
\end{aligned}$$

By changing the time scale, this gives the replicator equations. □

Now we obtain the non-local replicator equations using theorem given in the previous section and the equality (3.2.4).

$$\begin{aligned}
\frac{\partial u_i}{\partial t} &= \sum_{k\in S} r(x, k, i, \mathbf{u})u_k(x, t) - u_i(x, t) \sum_{k\in S} r(x, i, k, \mathbf{u}) \\
&= \sum_{k\in S} J * u_i[1 + w(\sum_l m_{il} J * u_l - \sum_l m_{kl} J * u_l)]u_k \\
&\quad -u_i \sum_{k\in S} J * u_k[\frac{1}{2} - w(\sum_l m_{il} J * u_l - \sum_l m_{kl} J * u_l)] \\
&= \sum_{k\in S} [(u_k J * u_i - u_i J * u_k) - w(u_k J * u_i + u_i J * u_k)(\sum_l m_{kl} J * u_l - \sum_l m_{il} J * u_l)]
\end{aligned}$$

We can further simplify this equation using $\sum_{k\in S} u_k = \sum_{k\in S} J * u_k = 1$. Then, we get

$$\frac{\partial u_i}{\partial t}(x,t) = J * u_i - u_i + w\Big[(J * u_i + u_i)\sum_{l\in S} m_{il} J * u_l - \sum_{k,l\in S} m_{kl}(u_k J * u_i + u_i J * u_k) J * u_l\Big]$$

Again if there is no spatial structure then by taking $u_i(x) = \rho_i$ we get $\int J(x-y)u_i(y)\,dy = \rho_i \int J(x-y)\,dy = \rho_i$. Thus, above equation reduces to replicator equation.

3.4.2 Proof of theorem 3.3.1

The following proposition gives the existence of monotone traveling waves that connect two equilibria of the traveling wave equation (3.3.3).

Proposition 3.4.5. *Suppose that J satisfies **J1**, $a \le 0$ and $1 > w(b-a)$, then traveling wave solutions of (3.3.3) exist for $c \ge c_0$.*

Proof. The existence of solutions to (3.3.3) was proved for $c > c_0^+$ in [46]. For $c < c_0^-$, it is easy to establish the same results by constructing appropriate sub and super solutions. We prove the existence of traveling waves for the critical speed $c = c_0^+$ following [6]. Suppose $c_n > c_0$ be a sequence of numbers such that $c_n \to c_0$ as $n \to \infty$. Let U_n denote the traveling wave solution of (6) with speed c_n. Thus, $0 \le U_n \le 1$ and the solution is uniformly bounded by existence of solutions. Using $\int_{\mathbb{R}} J(y)\,dy = 1$, it is easy to see $J * U$ is uniformly bounded by 1. Using these bounds, we can obtain

$$|U_n'| \le c_n^{-1}(|J * U_n| + |U_n| + wb|U_n + J * U_n|) \le 4c_n^{-1} \tag{3.4.2}$$

Hence, U' is also uniformly bounded.

Using Taylor expansion, we have: $|U_n(s) - U_n(t)| = |s-t||U_n'(\nu)|$ for some ν between s and t. By uniform boundedness of U', it follows that U_n is equicontinuous for all n. Now, consider $J * U_n$. If $|s-t| < \delta$ then $|J * U_n(s) - J * U_n(t)| \le \int_{\mathbb{R}} |U_n(s+y) - U_n(t+y)|J(y)\,dy \le \epsilon$ since U_n is equicontinuous. It is also easy to see equicontinuity of U_n' using the above results. Therefore, U_n, $J * U_n$ and U_n' are uniformly bounded and equicontinuous for all n.

Thus, by Arzela-Ascoli theorem, we have a subsequence of U_n such that U_{n_k}, $J * U_{n_k}$ and U_{n_k}' converges uniformly on every bounded interval. If we denote the limit of U_{n_k} by U then U is differentiable and $U_{n_k}' \to U'$ Similarly, $J * U_{n_k} \to J * U$. Then Taking the limit in (3.3.3) gives

$$-c_0 U' = J * U - U + w(U + J * U - 2UJ * U)(aJ * U_1 + b) \quad \text{as} \quad n \to \infty.$$

This implies that U is the solution satisfying equation (3.3.3) with speed c_0. □

The following result is a direct corollary of theorem 3.3.4.

Corollary 3.4.6. *If $c \in (c_0^-, c_0^+)$, there are no non-constant solutions of equation (3.3.3).*

3.4.3 Proof of theorem 3.3.2

Step 1: We work on the space of bounded uniformly continuous functions $X_T = BUC(\mathbb{R} \times [0,T])$ equipped with the norm

$$||v||_T = \sup_{(x,t)} |v(x,t)|.$$

For $v \in X_T$ such that $0 \le v \le 1$, let u be a solution to the following equation:

$$\frac{\partial}{\partial t}u = J * v - u + w(u + J * v - 2uJ * v)(aJ * v + b) \tag{3.4.3}$$

with the initial data

$$u = u_0 \quad \text{on} \quad \mathbb{R} \times \{0\}.$$

Clearly, $0 \le J * v \le 1$. If $u = 0$ at some point (x,t), then $\frac{\partial u}{\partial t} = J * v + wJ * v(bJ * v + a_2) \ge 0$. So the trajectory of u is always beyond 0. It can also be shown that $\dot{u} \le 0$ when u is 1. Hence, $u \in [0,1]$. Existence of such a solution can be proven by the Lipchitz continuity of the right hand side and Banach fixed point theorem.

Step 2: Let v_i, $i = 1,2$ be two functions in X_T and let u_i denote the corresponding solutions of equation (3.2.7) with the same initial data. Say $u = u_1 - u_2$ and $v = v_1 - v_2$ then u satisfies the equation

$$\frac{\partial}{\partial t}u = \Upsilon_1 u + \Upsilon_2 v \tag{3.4.4}$$

where $\Upsilon_1 = -(1 - bw - (aw - 2b)J * v_1 + 2aw(J * v)^2)$ and $\Upsilon_2 = 1 + bw + (aw - 2bw)u_2 + awJ * (v_1 + v_2) - 2awu_2 J * (v_1 + v_2)$. Integration up to time t yields

$$u \quad = \int_0^t \Upsilon_1 u \, ds + \int_0^t \Upsilon_2 v \, ds$$

. By taking the absolute value of both sides gives

$$|u| \quad \le \int_0^t |\Upsilon_1||u| \, ds + \int_0^t |\Upsilon_2||v| \, ds$$

Say $K_i = \max_{u_j, v_j \in [0,1]} \Upsilon_k$ for $i,j,k = 1,2$, then we get

$$|u| \le K_1 t||u||_t + K_2 t||v||_t.$$

Taking the supremum over $(x,t) \in \mathbb{R} \times [0,T]$, we get

$$||u||_T \leq \frac{TK_2}{1-TK_1}||v||_T.$$

For sufficiently small T, $\frac{TK_2}{1-TK_1} < 1$. This implies that $Tv = u$ is a contraction mapping. This guarantees the existence and uniqueness of the solution in $[0,T]$ and this result can be extended to larger intervals by continuity.

Step 3: Let u_i be the solutions of the equation (3.2.5) corresponding with the initial datum u_{0i} satisfying the hypotheses of the theorem, set $u = u_1 - u_2$. Then we get an equation of the form (3.4.4) with $\Upsilon_1 = -(1 - bw - (aw - 2b)J * u_1 + 2aw(J * u)^2)$ and $\Upsilon_2 = 1 + bw + (aw - 2bw)J * u_2 + awJ * (u_1 + u_2) - 2awu_2J * (u_1 + u_2)$. Multiplying this equation by $\text{sign}_+(u)$ and using the fact that $\Upsilon_2 > 0$ if **P1** holds, we get

$$u_+(x,t) \leq \frac{tK_2}{1-tK_1}\int_0^t J * u_+(x,s)\,ds \leq \frac{tK_2}{1-tK_1}||u_+||_t$$

Using the same argument as above, for small t, we have $\frac{tK_2}{1-tK_1} < 1$. It follows that $u_+ = 0$ in $[0,t]$ since $(u_{01} - u_{02})_+ = 0$. This result can be extended to all times by continuity.

3.4.4 Proof of lemma 3.3.4

Consider the characteristic equation

$$\Delta_c(s) = -cs + d_1M(s) - d_2 \tag{3.4.5}$$

defined on (s^-, s^+) for $d_1, d_2 > 0$. Then, we have $\Delta_c''(s) = \int_{\mathbb{R}} y^2 e^{sy} J(y)\,dy$. This implies $\Delta_c(s)$ is convex on $(0, s^+)$ and $(s^-, 0)$. Thus, for sufficiently large s^+ and s^-, there exist two unique points $s_0^+(d_1,d_2) < s^+$ and $s_0^-(d_1,d_2) > s^-$ such that $\Delta_c'(s_0^{\pm}(d_1,d_2)) = 0$ Therefore, $A(s) := \frac{1}{s}[d_1\int_{\mathbb{R}} J(y)e^{sy}\,dy - d_2]$ takes its maximum and minimum values at the points $s_0^{\mp}(d_1,d_2)$. Moreover, $A(s_0^{\pm}) = c_0^{\pm}(d_1,d_2)$. In addition, Δ_c is increasing (decreasing) function of d_1 (d_2) and is continuous in these parameters as long as $M(s)$ is defined. Suppose $d_1 \leq 1 + bw$ and $d_2 \geq 1 - bw$, then $c_0^{\pm}(d_1,d_2) \to c_0^{\pm}$ defined in (3.3.2) as $d_1 \to 1 + bw$ and $d_2 \to 1 - bw$

Lemma 3.4.7. *Let $c \in (c_0^-, c_0^+)$ be given. Then there exists a function $V(\xi)$ positive on $(0, \pi/\gamma)$ such that $Q_c[\epsilon V(\xi)] \geq 0$ and*

$$Q_c[\epsilon V] > 0 \quad \text{on} \quad (0, \pi/\gamma)$$

for sufficiently small $\epsilon, \gamma > 0$.

Proof. Take $V_0(\xi) = \exp(-s\xi)\sin(\gamma\xi)$ where $s \in S_0 = (-s_0^-, s_0^+)\backslash\{0\}$ and consider the linear equation $\frac{\partial u}{\partial t} = L_c[u] = u_\xi + d_1 J * u - d_2 u$. then $L_c[V_0](\xi)$ is given by

$$\begin{aligned} [\quad & -cs + d_1 \int_{\mathbb{R}} J(y) e^{sy} \cos(\gamma y)\, dy - d_2] V_0(\xi) \\ + \quad & [c\gamma - d_1 \int_{\mathbb{R}} J(y) e^{sy} \sin(\gamma y)\, dy] e^{-s\xi} \cos(\gamma\xi) \end{aligned}$$

Define the functions

$$\mathbb{A}(s,\gamma) = \frac{1}{s}[d_1 \int_{\mathbb{R}} J(y) e^{sy} \cos(\gamma y)\, dy - d_2] \tag{3.4.6}$$

$$\mathbb{B}(s,\gamma) = \frac{d_1}{\gamma}[\int_{\mathbb{R}} J(y) e^{sy} \sin(\gamma y)\, dy] \tag{3.4.7}$$

We want

$$\mathbb{A}(s,\gamma) > (<) c \text{ if } s > (<) 0 \quad \text{and} \quad c = \mathbb{B}(s,\gamma) \tag{3.4.8}$$

so that $L_c[V_0(\xi)] > 0$ on $(0, \frac{\pi}{\gamma})$. Denote the limits of these functions by $A(s)$ and $B(s)$ as $\gamma \to 0$. Convergence is uniform in any closed and bounded interval of S_0. $B(s)$ is increasing and differentiation of A gives $(B(s) - A(s))/s$. By assumptions, it is clear that $A(s) > \ (<)\ B(s)$ on $(0, s_0^+)$ (on $(s_0^-, 0)$). Thus, A is decreasing for $0 < s < s_0^+(d_1, d_2)$ and $s_0^-(d_1, d_2) < s < 0$. And clearly $B(s)$ is increasing on S_0. Moreover, $B(s_0^\pm(d_1, d_2)) = c_0^\pm(d_1, d_2) = A(s_0^\pm)$ implying $B(0) \in (c_0^-, c_0^+)$. Thus, for any $\delta > 0$ and arbitrarily chosen $c \in (c_0^-(d_1, d_2), B(0))$ we have

$$B(s_1) + \delta < c < B(s_2) - \delta$$

for sufficiently small γ and appropriately chosen s_1 and s_2. Thus there exist a $s(\gamma)$ such that $B(s(\gamma), \gamma) = c$. Clearly $A'(s)$ is negative and it implies $B(s) < A(s)$. Choose γ small enough to get $c = \mathbb{B}(s(\gamma), \gamma) < \mathbb{A}(s(\gamma), \gamma)$ so that (3.4.8) is satisfied. This implies $L_c[V_0] > 0$ in $(0, \pi/\gamma)$. Define

$$V(\xi) = \begin{cases} V_0(\xi) & \text{if } \xi \in (0, \pi/\gamma) \\ 0 & \text{if } \xi \notin (0, \pi/\gamma) \end{cases}$$

By lemma 2 of [2], it follows that $L_c[V] > 0$ on $\xi \in (0, \pi/\gamma)$. Now, show $Q_c(\epsilon V_0)$ is positive on $(0, \pi/\gamma)$. Choose two positive numbers $\varepsilon_1, \varepsilon_2$ small enough such that for any $c \in (c_0^-, c_0^+)$, c is also in $(c_0^-(d_1, d_2), c_0^+(d_1, d_2)$ where $(d_1, d_2) = (1 + cw - \varepsilon_1, 1 - bw + \varepsilon_2)$ due to continuity of (3.4.5). Then we can choose ϵ small enough to get $Q_c(\epsilon V_0) - L_c(\epsilon V_0) > 0$. Thus, $Q_c(\epsilon V) > L_c(\epsilon V) > 0$ on $(0, \pi/\gamma)$. $Q_c(\epsilon V_0) \geq 0$ follows from theorem 3.3.2 and above discussion. □

Suppose u is the solution of (3.3.4) and (3.3.5) with given initial data $\tilde{u}_0$, we can write these equations in the following integral form:

$$u(x,t) = u_0(x)e^{-(1-bw)t} + \int_0^t e^{-(1-bw)(t-s)}\mathbf{F}(u, J*u)(x,s)\,ds \tag{3.4.9}$$

and

$$u(\xi,t) = u_0(\xi - ct)e^{-(1-bw)t} + \int_0^t e^{-(1-bw)(t-s)}\mathbf{F}(u, J*u)(\xi - c(t-s), s)\,ds \tag{3.4.10}$$

.

Proposition 3.4.8. *Suppose **J1-J2** and **P1** hold. Then, the solution of the initial value problem*

$$\frac{\partial}{\partial t}u = Q_c[u]$$
$$u(\xi,0) = \epsilon V$$

satisfies $\lim_{t\to\infty} u(\xi,t) = 1$ *for* $c \in (c_0^-, c_0^+)$.

Proof. By theorem 3.3.2, $u(\xi,t) \le 1$. Therefore, the limit $\lim_{t\to\infty} u(\xi,t) = q(\xi)$ exists. Define a new variable of integration $\theta = \xi + c(t-\tau)$ to get

$$u(\xi,t) = \epsilon V_0(\xi - ct)e^{-(1-bw)t} + \frac{1}{c}\int_\xi^\infty e^{\frac{1-bw}{c}(\xi-\theta)}\mathbb{I}_{[\xi,\xi+ct]}\mathbf{F}(u, J*u)(\theta, t - \frac{1}{c}(\theta-\xi))\,d\theta. \tag{3.4.11}$$

where $\mathbb{I}$ denotes the indicator function. taking the limit as $t \to \infty$ gives the equation

$$q(\xi) = \frac{1}{c}\int_0^\infty e^{\frac{1-bw}{c}(\xi-\theta)}\mathbf{F}(q, J*q)(\theta)\,d\theta. \tag{3.4.12}$$

Taking the derivative gives

$$q' = \frac{1-bw}{c}q + \frac{1}{c}\mathbf{F}(q, J*q)$$

which is the steady state equation of (3.2.7). Moreover, this equation has the form of (3.3.3) having two constant solutions, 0 and 1. By above lemma, it is easy to conclude that $q(\xi) > \epsilon V$ in $[0, \pi/\gamma]$. In addition, proposition 1 of [2] states that $q > 0$. Using continuity of q concludes that $q(\xi + h) > \epsilon V$ in $[0, \pi/\gamma]$ and $q(\xi + h) \ge \epsilon V$ in $\mathbb{R}$ for sufficiently small h. We see that $q(\xi + h) \ge q(\xi)$ in $[0, \pi/\gamma]$ for small enough $h \in \mathbb{R}$ by comparison principle. This implies $q' = 0$ so q is a constant. q has to be 1 since $q > 0$ in $(0, \pi/\gamma)$. □

3.4.4.1 Proof of lemma 3.3.3

Let W be the solution of the initial value problem given in lemma 3.3.3. By proposition 1 of [2], there exists a time $T > 0$ such that

$$\min\{W(\xi, T)|0 \leq \ \xi < \frac{\pi}{\gamma}\} = m > 0.$$

Choose ϵ small enough such that $\epsilon V \leq m$ in $[0, \pi/\gamma]$. Suppose $u(\xi, t)$ is the corresponding initial value problem as in proposition 3.4.8. Then $u(\xi, 0) \leq W(\xi, T)$. It follows from the comparison lemma that $u(\xi, t - T) \leq W(\xi, t)$ for all t. Since $u(\xi, \infty) = 1$, $W(\xi, \infty) = 1$

3.4.5 Proof of theorem 3.3.4

First, we show that the spreading speeds defined in (3.3.6) are finite. To this extend, we need following definition:

Definition 3.4.9. (sub and super-solutions) Consider the equation $u_t = f(u, J * u)$. A function $\omega = \bar{u}\ (\underline{u}) \in BUC(\mathbb{R} \times \mathbb{R}^+)$ is said to be a super(sub)-solution of the equation if it has left partial derivative with respect to t such that

$$\frac{\partial \omega}{\partial t-} \geq \ (\leq) f(\omega, J * \omega)$$

Proposition 3.4.10. *Spreading speeds defined in* (3.3.6) *are finite.*

Proof. The solution to equation (3.2.7) takes values in between 0 and 1. Thus, we can find two numbers d_1 and d_2 such that $H[u] \leq d_1 u + d_2 J * u$. For these values of d_i, we get the roots of the characteristic equation (3.4.5) as $c^{\pm} := c_0^{\pm}(d_1, d_2)$ It is easy to verify that the function

$$\omega(x, t) = \min\{1, Ke^{x + c^{\pm} t}\}$$

is a super-solution of the equation (3.2.7). Suppose u_0 is the initial condition of the equation with compact support. Choose K such that $0 \leq u_0(x) \leq \omega(x, 0)$, then by comparison principle $u(\xi, t) \leq \omega(\xi, t) \to 0$ as $t \to \infty$ for $|c| \geq c^{\pm}$. This implies $c_*^+ \leq c^+$ and $c_*^- \geq c^-$. □

Now we need to show that $c_*^{\pm}$ are spreading speeds. It is clear,by definition, that $\lim_{t \to 0} u(x + ct, t) = 1$ if $c \in (c_*^-, c_*^+)$ and $\lim_{t \to 0} u(x + ct, t) \neq 1$ otherwise. Denote the solution to equation (3.2.7) as $u_n(x) = u(x, n)$ for $n \in \mathbb{N}$. Then u_n satisfies the recursion

$$u_n(x) = Q[u_{n-1}](x)$$

Clearly, we get the order preserving property for this operator as a result of comparison principle. In addition, the operator is translation invariant i.e $T_y[Q[u]] = Q[T_y[u]]$ for any $y \in \mathbb{R}$. We refer the proof of Lemma 3.1 given in [54] to prove the continuity of the operator.

Moreover, $Q^{(n)}[\alpha] \to 1$ as $n \to \infty$ for any $0 < \alpha < 1$ by lemma 3.3.3 and the hypothesis of the theorem $0 \in (c_0^-.c_0^+)$.

Thus, we see that $\lim u(x + ct, t) = 0$ or 1 by theorems 3.1 and 3.2 in [29].

The last statement $c_0^{\pm} = c_*^{\pm}$ follows from the fact that if $a < 0$ then $H[u] \leq \mathcal{M}[u]$. This allows us to choose $d_1 = 1 + bw$ and $d_2 = -1 + bw$ in proposition 3.4.10. Combining this with lemma 3.3.3 gives the desired result.

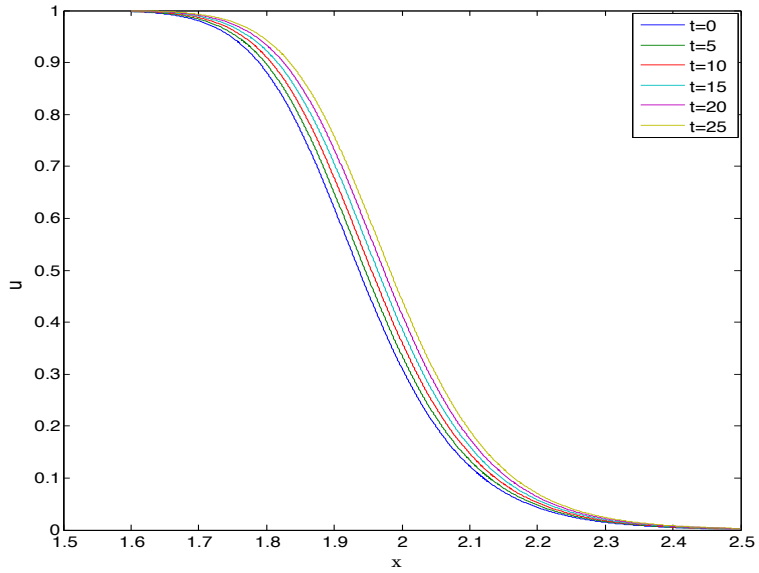

(a) Spread of defectors for $a = 0.999$

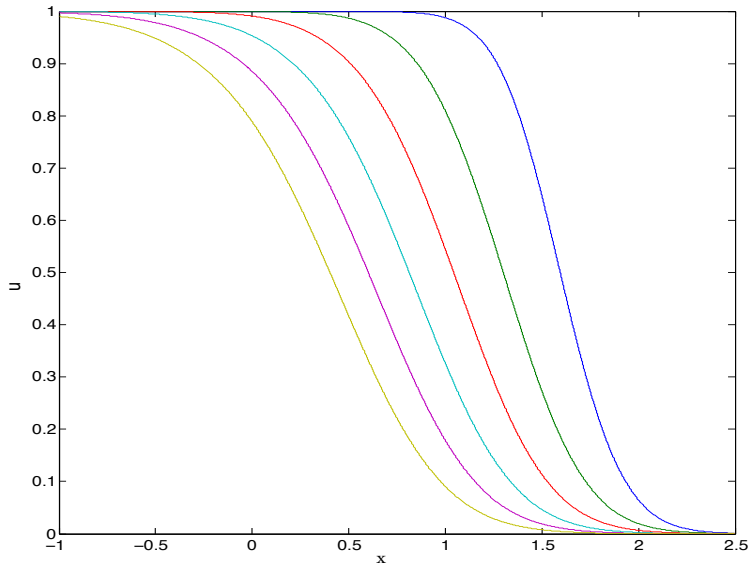

(b) Cooperators take over the population for $a = 0$

Figure 3.3 Asymptotic behavior of defectors for the game with parameters $w = 1$, $b = 0.1$, $\sigma = 0.1$ and $c = 0.095$ is shown. Successive solutions are separated by 5 time units. 40000− points were used in the spatial domain $[-40, 40]$ and the step size for spatial domain was 0.002. Time step was chosen as 0.0005. The initial condition is the blue curve shown in the figure with support $[-2.5, 2.5]$.

BIBLIOGRAPHY

[1] J.C. Allen, C.C. Brewster, and D.H. Slone. Spatially explicit ecological models: a spatial convolution approach. *Chaos, Solitons & Fractals*, 12(2):333–347, 2001.

[2] D.G. Aronson. The asymptotic speed of propagation of a simple epidemic. *Nonlinear Diffusion*, 14:1–23, 1977.

[3] D.G. Aronson and H.F. Weinberger. Nonlinear diffusion in population genetics, combustion, and nerve pulse propagation. *Partial Differential Equations and Related Topics*, pages 5–49, 1975.

[4] R. Axelrod. *The evolution of cooperation: revised edition*. Basic Books, 2006.

[5] M. Benaïm and J.W. Weibull. Deterministic approximation of stochastic evolution in games. *Econometrica*, 71(3):873–903, 2003.

[6] K.J. Brown and J. Carr. Deterministic epidemic waves of critical velocity. *Math. Proc. Cambridge Philos. Soc*, 81:431–433, 1977.

[7] L. Cao, H. Ohtsuki, B. Wang, and K. Aihara. Evolution of cooperation on adaptively weighted networks. *Journal of Theoretical Biology*, 272(1):8–15, 2011.

[8] H. Caswell. *Matrix population models*. Wiley Online Library, 2006.

[9] P. Chesson and C.T. Lee. Families of discrete kernels for modeling dispersal. *Theoretical Population Biology*, 67(4):241–256, 2005.

[10] J.S. Clark, M. Silman, R. Kern, E. Macklin, and J. HilleRisLambers. Seed dispersal near and far: patterns across temperate and tropical forests. *Ecology*, 80(5):1475–1494, 1999.

[11] H. Cramer. *Mathematical Methods of Statistics (PMS-9)*, volume 9. Princeton University Press, 1999.

[12] M. Doebeli, C. Hauert, and T. Killingback. The evolutionary origin of cooperators and defectors. *Science*, 306(5697):859–862, 2004.

[13] R.S. Etienne and J. Rosindell. The spatial limitations of current neutral models of biodiversity. *PloS one*, 6(3):e14717, 2011.

[14] C. Grilo and L. Correia. Effects of asynchronism on evolutionary games. *Journal of Theoretical Biology*, 269(1):109–122, 2011.

[15] W.D. Hamilton and R. Axelrod. The evolution of cooperation. *Science*, 211(27):1390–1396, 1981.

[16] C. Hauert. Effects of space in 2×2 games. *International Journal of Bifurcation and Chaos*, 12(07):1531–1548, 2002.

[17] C. Hauert and M. Doebeli. Spatial structure often inhibits the evolution of cooperation in the snowdrift game. *Nature*, 428(6983):643–646, 2004.

[18] J. Hofbauer. Equilibrium selection via traveling waves. *Yearbook of the Institute Vienna Circle*, 5(97):245–260, 1998.

[19] J. Hofbauer, V. Hutson, and G.T. Vickers. Traveling waves for games in economics and biology. *Nonlinear Analysis, Theory, Methods & Applications*, 30:1235–1244, 1997.

[20] J. Hofbauer and K. Sigmund. *Evolutionary games and population dynamics*. Number Cambridge. Cambridge University Press, 1998.

[21] V. Hutson and G.T. Vickers. Traveling waves and dominance of ess's. *Journal of Mathematical Biology*, 30(5):457–471, 1992.

[22] S.H. Hwang. *Spatial Evolutionary Game Theory: Deterministic Approximations, Decompositions, and Hierarchical Multi-scale Models*. PhD thesis, University of Massachusetts - Amherst, 2011.

[23] S.H. Hwang, M. Katsoulakis, and L. Rey-Bellet. Deterministic equations for stochastic spatial evolutionary games. *arXiv preprint arXiv:1007.0723*, 2010.

[24] M. Ifti, T. Killingback, and M. Doebeli. Effects of neighborhood size and connectivity on spatial continuous prisoner's dilemma. *arXiv preprint q-bio/0405018*, 2004.

[25] M. Kot, M.A. Lewis, and P. van den Driessche. Dispersal data and the spread of invading organisms. *Ecology*, 77(7):2027–2042, 1996.

[26] Y. Kuang. *Delay differential equations: with applications in population dynamics*, volume 191. Academic Press, 1993.

[27] H. Kuraoka, N. Fujii, and K. Ueda. Emergence of cooperation in a network environment introducing social distance. In *Proceedings of European Conference on Complex Systems (ECCS'06)*, 2006.

[28] E. Lieberman, C. Hauert, and M.A. Nowak. Evolutionary dynamics on graphs. *Nature*, 433(7023):312–316, 2005.

[29] R. Lui. Biological growth and spread modeled by systems of recursions. i. mathematical theory. *Mathematical Biosciences*, 93(2):269–295, 1989.

[30] F. Lutscher, E. Pachepsky, and M.A. Lewis. The effect of dispersal patterns on stream populations. *SIAM Journal on Applied Mathematics*, 65(4):1305–1327, 2005.

[31] S. Ma, P. Weng, and X. Zou. Asymptotic speed of propagation and traveling wavefronts in a non-local delayed lattice differential equation. *Nonlinear Analysis: Theory, Methods & Applications*, 65(10):1858–1890, 2006.

[32] R.M. May. More evolution of cooperation. *Nature*, 327:15–17, 1987.

[33] J. Medlock and M. Kot. Spreading disease: integro-differential equations old and new. *Mathematical Biosciences*, 184(2):201–222, 2003.

[34] R. Muneepeerakul, S. Azaele, S.A. Levin, A. Rinaldo, and I. Rodriguez-Iturbe. Evolution of dispersal in explicitly spatial metacommunities. *Journal of Theoretical Biology*, 2010.

[35] M.A. Nowak, S. Bonhoeffer, and R.M. May. More spatial games. *International Journal of Bifurcation and Chaos*, 4(1):33–56, 1994.

[36] M.A. Nowak and R.M. May. Evolutionary games and spatial chaos. *Nature*, 359(6398):826–829, 1992.

[37] M.A. Nowak and M. Robert. The spatial dilemmas of evolution. *International Journal of Bifurcation and Chaos*, 3(01):35–78, 1993.

[38] M.A. Nowak and K. Sigmund. Games on grids. *The Geometry of Ecological interactions: Simplifying Spatial Complexity*, pages 135–150, 2000.

[39] H. Ohtsuki, C. Hauert, E. Lieberman, and M.A. Nowak. A simple rule for the evolution of cooperation on graphs and social networks. *Nature*, 441(7092):502–505, 2006.

[40] M. Perc and A. Szolnoki. Coevolutionary games-a mini review. *Biosystems*, 99:109–125, 2010.

[41] W.H. Press and F.J. Dyson. Iterated prisoner's dilemma contains strategies that dominate any evolutionary opponent. *Proceedings of the National Academy of Sciences*, 109(26):10409–10413, 2012.

[42] E. Presutti. *Scaling limits in statistical mechanics and microstructures in continuum mechanics*. Springer, 2008.

[43] D.C. Queller. A general model for kin selection. *Evolution*, pages 376–380, 1992.

[44] B.D. Ripley. *Spatial statistics*, volume 575. Wiley-Interscience, 2005.

[45] C.P. Roca, J.A. Cuesta, and A. Sánchez. Effect of spatial structure on the evolution of cooperation. *Physical Review E*, 80(4):046106, 2009.

[46] K. Schumacher. Traveling-front solutions for integro-differential equations. *IJ Reine Angew. Math*, 316:54–70, 1980.

[47] L.H. Shang, X. Li, and X.F. Wang. Cooperative dynamics of snowdrift game on spatial distance-dependent small-world networks. *The European Physical Journal B-Condensed Matter and Complex Systems*, 54(3):369–373, 2006.

[48] D.H. Slone. Increasing accuracy of dispersal kernels in grid-based population models. *Ecological Modeling*, 222(3):573–579, 2011.

[49] J.M. Smith and G.R. Price. The logic of animal conflict. *Nature*, 246:15, 1973.

[50] J.M. Smith and E. Szathmary. *The major transitions in evolution*. Oxford University Press, 1997.

[51] M.B. Soons, G.W. Heil, R. Nathan, and G.G. Katul. Determinants of long-distance seed dispersal by wind in grasslands. *Ecology*, 85(11):3056–3068, 2004.

[52] S. Számadó, F. Szalai, I. Scheuring, et al. The effect of dispersal and neighborhood in games of cooperation. *Journal of Theoretical Biology*, 253(2):221, 2008.

[53] A. Traulsen, J.C. Claussen, and C. Hauert. Coevolutionary dynamics: from finite to infinite populations. *Physical Review Letters*, 95(23):238701, 2005.

[54] P. Weng and X. Zhao. Spreading speed and traveling waves for a multi-type sis epidemic model. *Journal of Differential Equations*, 229(1):270–296, 2006.

[55] H.P. Young. *Individual strategy and social structure: An evolutionary theory of institutions*. Princeton University Press, 2001.